Ancient sedimentary DNA shows rapid post-glacial colonisation of Iceland followed by relatively stable vegetation until Landnám

Inger Greve Alsos, Youri Lammers, Sofia E. Kjellman, Marie Kristine Føreid Merkel, Emma M. Bender, Alexandra Rouillard, Egill Erlendsson, Esther Ruth Guðmundsdóttir, Ívar Örn Benediktsson, Wesley R. Farnsworth, Skafti Brynjólfsson, Guðrún Gísladóttir, Sigrún Dögg Eddudóttir, Anders Schomacker

Corresponding author: Inger Greve Alsos, inger.g.alsos@uit.no

Inger Greve Alsos, Tromsø University Museum, UiT The Arctic University of Norway, NO-9037 Tromsø, Norway. https://orcid.org/0000-0002-8610-1085, inger.g.alsos@uit.no

Youri Lammers, Tromsø University Museum, UiT The Arctic University of Norway, NO-9037 Tromsø, Norway. https://orcid.org/0000-0003-0952-2668, youri.lammers@uit.no

Sofia E. Kjellman, Department of Geosciences, UiT The Arctic University of Norway, P.O. Box 6050 Langnes, NO-9037 Tromsø, Norway. https://orcid.org/0000-0003-1165-8601, sofia.e.kjellman@uit.no

Marie Kristine Føreid Merkel, Tromsø University Museum, UiT The Arctic University of Norway, NO-9037 Tromsø, Norway, marie.f.merkel@uit.no.

Emma M. Bender, Department of Geosciences, UiT The Arctic University of Norway, P.O. Box 6050 Langnes, NO-9037 Tromsø, Norway. emma.bender@online.de

Alexandra Rouillard, Department of Geosciences, UiT The Arctic University of Norway, P.O. Box 6050 Langnes, NO-9037 Tromsø, Norway and Section for GeoGenetics, GLOBE Institute, University of Copenhagen, Øster Voldgade 5-7, DK-1350 Copenhagen K., Denmark. https://orcid.org/0000-0001-5778-6620, alexandra.rouillard@uit.no

Egill Erlendsson, Institute of Life and Environmental Sciences, University of Iceland, Askja, Sturlugata 7, IS-102 Reykjavík, Iceland. https://orcid.org/0000-0002-2264-3504, egille@hi.is.

Esther Ruth Guðmundsdóttir, Department of Geosciences, UiT The Arctic University of Norway, P.O. Box 6050 Langnes, N-9037 Tromsø and Institute of Earth Sciences, Nordic Volcanological Center, University of Iceland, Askja, Sturlugata 7, IS-102 Reykjavík, Iceland. https://orcid.org/0000-0001-6987-3641, estherrg@hi.is

Ívar Örn Benediktsson, Institute of Earth Sciences, University of Iceland, Askja, Sturlugata 7, IS-102 Reykjavík, Iceland. https://orcid.org/0000-0002-9966-0767, ivarben@hi.is

Wesley R. Farnsworth, NordVulk, Nordic Volcanological Center, University of Iceland, Askja, Sturlugata 7, IS-102 Reykjavík, Iceland. https://orcid.org/0000-0001-7375-2228, wesleyf@hi.is

Skafti Brynjólfsson, Icelandic Institute of Natural History, Borgum við Norðurslóð, IS-600 Akureyri, Iceland. https://orcid.org/0000-0002-2792-1964, skafti@ni.is

Guðrún Gísladóttir, Institute of Life and Environmental Sciences and Institute of Earth Sciences, University of Iceland, Askja, Sturlugata 7, IS-102 Reykjavík, Iceland. https://orcid.org/0000-0002-4309-2414, ggisla@hi.is

Sigrún Dögg Eddudóttir, University of Uppsala, Department of Archaeology and Ancient History, Engelska parken, Thunbergsvägen 3H, Box 626, 751 26 Uppsala, Sweden. https://orcid.org/0000-0002-8632-8191, sigrun.dogg.eddudottir@arkeologi.uu.se

Anders Schomacker, Department of Geosciences, UiT The Arctic University of Norway, P.O. Box 6050 Langnes, NO-9037 Tromsø, Norway. https://orcid.org/0000-0002-8031-9008, anders.schomacker@uit.no

Abstract

Understanding patterns of colonisation is important for explaining both the distribution of single species and anticipating how ecosystems may respond to global warming. Insular flora may be especially vulnerable because oceans represent severe dispersal barriers. Here we analyse two lake sediment cores from Iceland for ancient sedimentary DNA to infer patterns of colonisation and Holocene vegetation development. Our cores from lakes Torfdalsvatn and Nykurvatn span the last *c*. 12,000 cal. yr BP and *c*. 8600 cal. yr BP, respectively. With near-centennial resolution, we identified a total of 191 plant taxa, with 152 taxa identified in the sedimentary record of Torfdalsvatn and 172 plant taxa in the sedimentary record of Nykurvatn. The terrestrial vegetation at Torfdalsvatn was first dominated by bryophytes, arctic herbs such as *Saxifraga* spp. and grasses. Around 10,100 cal. yr BP, a massive immigration of new taxa was observed, and shrubs and dwarf shrubs became common whereas aquatic macrophytes became dominant. At Nykurvatn, all dominant taxa occurred already in the earliest samples; shrubs and dwarf shrubs were more abundant at this site than at Torfdalsvatn. There was an overall steep increase both in the local and regional species pool until 8000 cal. yr BP, by which time ¾ of all taxa identified had arrived. In the period 4500-1000 cal. yr BP, a few new taxa of bryophytes, graminoids and forbs are identified. The last millennium, after human settlement of the island (Landnám), is characterised by a sudden disappearance of *Juniperus communis*, but also reappearance of some high arctic forbs and dwarf shrubs. Notable immigration during the Holocene coincides with periods of dense sea-ice cover, and we hypothesise that this may have acted as a dispersal vector. Thus, although ongoing climate change might provide a suitable habitat in Iceland for a large range of species only found in the neighbouring regions today, the reduction of sea ice may in fact limit the natural colonisation of new plant species.

Keywords

ancient DNA, colonisation, Holocene, island, lake sediments, metabarcoding, vegetation history

1. Introduction

Island biota are particularly vulnerable to climate change due to dispersal limitations (Harter et al., 2015; Weigelt et al., 2016). Because of arctic amplification, the earliest and most severe impact of climate change is expected at high latitudes (Bjorkman et al., 2018; CAFF, 2013). Subsequently, the fate of the flora in this region will depend on the species' ability to track this change. While the arctic flora is assumed to have frequent long-distance dispersal (Alsos et al., 2015, 2007), oceans represent the greatest dispersal barriers (Eidesen et al., 2013). Studies of contemporary vegetation as well as modelling simulations suggest a legacy of glaciation on patterns of taxonomic richness (Stewart et al., 2016; Svenning et al., 2015), whereas pollen records indicate either Early Holocene species saturation (Giesecke et al., 2019, 2012) or dispersal lags (Felde et al., 2018). Studies of ancient DNA may shed new light on this debate as it better detects taxa and provides a higher taxonomic resolution, thereby providing a stronger method to track past species occurrence (Clarke et al., 2020; Liu et al., 2020; Rijal et al., 2020). A recent study of ancient DNA in northern Fennoscandia suggests severe dispersal lags (Rijal et al., 2020), challenging our view of a very mobile arctic flora.

Iceland is among the most isolated islands in the North Atlantic. Glacial geological evidence and numerical modelling indicate that the last Icelandic Ice Sheet reached the shelf around Iceland during the Last Glacial Maximum (LGM) (Norðdahl and Ingólfsson, 2015; Patton et

al., 2017). While the renowned symposium in Iceland in 1962 (Löve and Löve, 1963) concluded that the majority of the biota must have survived the LGM *in situ*, later studies focusing on patterns of endemism and phylogeographic concluded that most species immigrated postglacially (Alsos et al., 2015; Brochmann et al., 2003). Furthermore, the estimated rate of colonisation in Iceland (1:33-214 yrs) is far greater than the Azores (1:40,000 yrs) or Hawaii (1:20,000-250,000 yrs; Alsos et al., 2015; Schaefer, 2003; Sohmer and Gustafson, 1987). Thus, the current view is that long-distance dispersal has been frequent in the amphi-Atlantic region. However, studies of phylogeography do not allow any direct dating of events, and older surviving populations may be swamped by new immigrants.

Palaeoecological data may provide more direct evidence of species at a given time and space. There are palaeoecological studies from ~70 profiles from ~36 sites in Iceland, the majority of them are pollen studies of peat deposits, only covering portions of the Holocene (Geirsdóttir et al., 2020; Hallsdóttir and Caseldine, 2005). Based on a review of all these records, the first occurrence could be determined for only 52 of 430 vascular plant taxa (Alsos et al., 2016). The average arrival date was 11,050 cal. yr BP, with a range from 13,000-7000 cal. yr BP. This average arrival date coincides with a period characterised by a high concentration of sea ice from the different source regions. Further, a close link was found between sea ice and driftwood. Thus, we hypothesise that sea-ice rafting was likely an important dispersal mechanism. Sea ice may act as a bridge, which allowed the Arctic fox to migrate to Iceland, potentially carrying seeds in the fur or digestive system (Graae et al., 2004). Also, it provided a smooth surface which seeds could have been wind-carried over. Furthermore, it may act as a ferry, transporting debris, driftwood and potentially propagules attached to it (Johansen and Hytteborn, 2001; Panagiotakopulu, 2014; Savile, 1972). However, determining the first arrival date for more taxa is needed to test this hypothesis.

The oldest post-glacial palaeoecological record from Iceland is from Lake Torfdalsvatn on the Skagi peninsula. The rich pollen and macrofossil record shows a relatively diverse arctic vegetation from 13,000 cal. yr BP, with more than ten taxa surviving the Younger Dryas, indicating that these species would also be able to survive the LGM *in situ* (Rundgren, 1998, 1995; Rundgren and Ingólfsson, 1999). From around 11,300 cal. yr BP, indicators of disturbed ground like *Oxyria/Rumex* and *Koenigia* are found together with *Betula,* as well as scattered records of *Salix* and *Empetrum* (Rundgren, 1998; Rundgren and Ingólfsson, 1999). A rapid Early Holocene warming led to exposure of land and development of soils 10,500-8500 cal. yr BP (Langdon et al., 2010). The Saksunarvatn tephra (10,200 cal. yr BP) marks the transition from the Preboreal to the Boreal period, and is suggested to have temporarily reduced the vegetation diversity and pollen concentrations (Rundgren, 1998). Burial by the tephra and subsequent aeolian processes are thought to have altered vegetation communities towards species more tolerant of sand burial (Eddudóttir et al., 2015). However, pollen records indicate a recovery towards pre-deposition vegetation communities within 100 years (Caseldine et al., 2006; Eddudóttir et al., 2015; Rundgren, 1998). An increase in pollen concentrations as well as a shift from grass dominance to *Salix* occurs during the early Boreal period. This is followed by a shift to dominance of *Juniperus communis* together with *Betula nana* and *Empetrum*, until birch woodland developed from 9400-6850 cal. yr BP (Eddudóttir et al., 2015; Hallsdóttir and Caseldine, 2005; Rundgren, 1998). During the Middle to Late Holocene, woodland became more patchy or open, while heath and mires expanded from around 7000 cal. yr BP (Eddudóttir et al., 2015; Hallsdóttir and Caseldine, 2005). The Norse settlement (Landnám) from around AD 870 was a rapid process, and by AD 930, most of the farmable land was claimed (Smith, 1995; Vésteinsson and McGovern, 2012). Landnám is characterised by a rapid decline in birch pollen, especially in the lowlands (Erlendsson, 2007;

158 Hallsdóttir, 1987; Hallsdóttir and Caseldine, 2005). This pattern is also found in the less
159 studied highlands (Eddudóttir et al., 2020), although some northeastern sites show decrease in
160 birch prior to Landnám (Roy et al., 2018). Following settlement, the vegetation changed due
161 to introduced plant species, habitat diversification as a result of land-use (mainly grazing), soil
162 erosion and increased landscape openness, and diminished competition from dominant species
163 (mainly birch). Such environmental modifications have almost certainly led to altered local
164 plant composition and landscape-scale distribution patterns of vegetation, and may explain
165 increased palynological richness near farms following Landnám (Erlendsson, 2007; Möckel et
166 al., 2017; Þórhallsdóttir, 1996).
167
168 Here we study sedimentary ancient DNA (*sed*aDNA) of two lakes to explore patterns of
169 species arrival and vegetation development over the Holocene. We investigate the lowland
170 Lake Torfdalsvatn, as it holds the oldest known lacustrine sedimentary record from Iceland
171 (Axford et al., 2007; Björck et al., 1992; Rundgren, 1998, 1995; Rundgren and Ingólfsson,
172 1999). Furthermore, sedimentary algal pigments, stable isotopes, and biogenic silica have
173 been analysed from the lake record (Florian, 2016). Lake Nykurvatn is located in a higher
174 elevation catchment and represents a less studied region of Iceland. Unlike Torfdalsvatn, the
175 site likely deglaciated during the Early Holocene (Norðdahl and Ingólfsson, 2015; Patton et
176 al., 2017). We focus on 1) the proportion and functional type of species present prior to the
177 onset of Early Holocene warming, which could indicate glacial survival, 2) patterns of arrival
178 for plants of different functional groups, and 3) any modification of the vegetation related to
179 Landnám.
180
181

182 ## 2.1. Torfdalsvatn, North Iceland

183 Torfdalsvatn (66.06°N, 20.38°W, 40 m a.s.l.) is located at the Skagi peninsula in North
184 Iceland (Fig. 1). The northern part of Skagi is characterised by gently undulating terrain with
185 thin sediment cover. From 1961-1990, the mean annual air temperature at Hraun located on
186 Skagi was 2.5°C, and the mean annual precipitation was 475 mm. In July, the mean air
187 temperature at Hraun was 8.2°C (Icelandic Meteorological Office, 2020a).
188
189 Torfdalsvatn has an area of 0.4 km^2 (Fig. 2), a catchment of *c*. 3.7 km^2 (Rundgren, 1995) and
190 a median slope of 1.1° (Florian, 2016). The water depth at the centre of the basin is *c*. 5.1 m
191 (Rundgren and Ingólfsson, 1999) to 5.8 m (Florian, 2016). Dwarf-shrub heaths, herb and
192 grass tundra, and *Carex*-dominated fens characterise the vegetation in the modern catchment
193 (Rundgren, 1997). The most abundant dwarf-shrub species are *Empetrum nigrum* and *Salix*
194 *herbacea,* and the shrub *Betula nana* is also common. (Björck et al., 1992) obtained an 11.95
195 m long sediment sequence from Torfdalsvatn, and showed that the sedimentary record goes
196 back to the Allerød, and that the site was ice free during the Younger Dryas. Palaeobotanical
197 data indicate a sparse to discontinuous cover of graminoids, herbs, shrubs and dwarf shrubs
198 during Allerød (Rundgren, 1997). During the Younger Dryas, the shrub and dwarf-shrub
199 vegetation disappeared, and the plant cover was sparse. In the Preboreal, the graminoids,
200 shrubs and dwarf shrubs reappeared.
201
202 Torfdalsvatn is shared between the landholdings of the active farms Tjörn and Hafnir. The
203 farms are both featured in a letter from AD 1285 regarding land boundaries of farms owned
204 by the Þingeyrarklaustur monastery (DI, 1857-1986, pp. 249-250). In *Jarðabók*, a land
205 registry from the beginning of the 18th century, the farms were still operating. Livestock
206 consisted of cattle, sheep and horses. Both farms also had access to *rifhrís* (*Betula nana*) for

207 firewood (Magnússon and Vídalín, 1927, pp. 473-479). Throughout, the inhabitants of both
208 farms have probably operated a standard pastoral farming.
209
210
211 ## 2.2. Nykurvatn, Northeast Iceland
212 Nykurvatn (65.63°N, 15.14°W, 428 m a.s.l.) is situated at the Bustarfell plateau above the
213 Hofsárdalur valley, located in the up to 20-km wide Vopnafjörður fjord-valley system in
214 Northeast Iceland (Fig. 1). The minimum age of deglaciation of the highland plateaus above
215 the Hofsárdalur valley is 9400 cal. yr BP (Sæmundsson, 1995). From 1995-2019, the mean
216 annual air temperature and precipitation at Skjaldþingsstaðir (42 m a.s.l.) in the Hofsárdalur
217 valley, 16 km northeast of Nykurvatn, are 3.8°C and 1215 mm, respectively. The July mean
218 temperature was 10.0°C (Icelandic Meteorological Office, 2020b). Nykurvatn has an area of
219 0.59 km^2 (Fig. 2), the catchment is *c*. 10 km^2, and the water depth at the centre of the lake is *c*.
220 10.0 m. The area around Nykurvatn is classified as moors and heathland (National Land
221 Survey of Iceland, 2020).
222
223 Ownership of Nykurvatn is shared between three currently occupied farmlands, Hauksstaðir,
224 Teigur and Bustarfell. Place names and house ruins indicate a greater density of farms and
225 cottages in the past. The adjacent farm Hof is listed in *Landnámabók* (Book of Settlements)
226 among the earliest settled farms (Benediktsson, 1968, p. 290) and Hauksstaðir (Haugsstaðir)
227 and Bustarfell enter the historical records no later than in the 14th century AD. Place names
228 and historical sources also attest to the existence of woodlands in the past (DI IV, p. 217).
229 Given the high altitude of Nykurvatn, summer grazing of livestock probably took place by the
230 lake.
231

3. Methods

3.1. Sediment coring and subsampling

Lake sediment cores were retrieved using a hand-held piston corer (150 and 200 cm long and 75 and 60 mm diameter coring tubes for Torfdalsvatn and Nykurvatn, respectively) from the lake ice. Seven core sections were collected from Torfdalsvatn (TDV2-1 to TDV2-7; water depth 5.1 m) in 2012. TDV core sections were purposely collected without overlap. Four overlapping core sections (NYK1 to NYK4; water depth 10.0 m) were collected in the centre of Nykurvatn in 2018. Additionally, one core (NYK5; water depth 3.8 m) was sampled in the distal (NE) end of the lake where the sedimentation rate is lower. The aim of this was to obtain older sediments because coring deeper below NYK4 was not possible with the piston corer. Cores were preserved in the dark and cold (~4°C) until opening.

Half-cores were sub-sampled for *sed*aDNA immediately upon opening, wearing full bodysuits, masks and sterile gloves in dedicated clean-lab facilities with no-PCR products. The TDV cores were sampled using 5 mL sterile disposable syringes as described by Voldstad et al. (2020) whereas the NYK core was sampled using clean disposable plastic knives and spatulas as described in Rijal et al. (2020). All samples were stored at 4°C until DNA extractions.

3.2 Geochemical analyses

The TDV cores were logged and analysed in the sediment lab and ITRAX core facility at the University of Copenhagen (Centre for GeoGenetics) and the NYK cores at UiT The Arctic University of Norway (Department of Geosciences). ITRAX and Avaatech core scanners were used to collect high-resolution data (X-ray fluorescence, (XRF), magnetic susceptibility

(MS), and optical and radiographic images) from split core sections from TDV and NYK, respectively. XRF measurements were conducted every 1 mm at 30 kV and 30 µA with a 30 s exposure for the ITRAX scanner and every 2 mm at 10 kV and 30 µA with a 20 s exposure time for the Avaatech scanner. Both core scanners have an X-ray source with a Rh (rhodium) anode (Croudace et al., 2006; Forwick, 2013). For the ITRAX measurements, Ti was normalised against the incoherent (inc) and coherent (coh) Rh scatter (Ti/(inc+coh)) to remove instrumental effects (Kylander et al., 2011). The Ti signal from the Avaatech scanner was normalised against the sum of Al, Si, S, K, Ca, Ti, Mn and Fe (Ti/Sum) to minimise artefacts (Weltje and Tjallingii, 2008). The Ti signal of the NYK core sections is presented to identify the overlap between core sections (Supplementary Fig. S1). Loss on ignition (LOI; Heiri et al., 2001) was measured to determine the total organic content for the NYK core. Samples (2 cm^3) were collected every 5 cm, with additional samples at visible transitions in the lithology. The samples were dried at 110°C for 2 h and ignited at 550°C for 4 h.

3.3 Age-depth modeling and core correlation

The chronologies of both lake cores were constructed based on accelerator mass spectrometry (AMS) ^{14}C measurements on plant macrofossils and identified tephra markers. The ^{14}C samples were analysed at the Ångström Laboratory, Uppsala University, Sweden. For calibrating the ^{14}C ages, the online OxCal software (v.4.4, Bronk Ramsey, 2009) and the IntCal20 dataset (Reimer et al., 2020) were used. All calibrated radiocarbon ages are presented as calibrated year before present (cal. yr BP; BP = 1950). Visually identified tephra layers were sampled and analysed for major element composition at the Institute of Earth Science, University of Iceland, using Electron Probe Microanalysis (EPMA). A JEOL JXA-8230 Super probe with an acceleration voltage of 15 kV, a beam current of 10 nA and a beam diameter of 10 µm was used for the EPMA. Natural and synthetic minerals were used for

standardisation as well as basaltic (A99) and rhyolitic glass (Lipari Obsidian; ATHO). On each polished thin section, 20-30 point analyses were performed on randomly selected lines. The dataset was examined for outliers and contamination by microlites. All analyses with sums lower than 95% were discarded. Tephra layers were identified based on their chemical composition.

The NYK1-NYK4 core sections were stratigraphically correlated based on identified tephra marker layers, ^{14}C ages, trends in the XRF data and visual similarities in lithology. Tie points were used to align the cores in AnalySeries (v. 2.0.4.2, Paillard et al., 1996) and construct a common stratigraphic depth-scale (Supplementary Fig. S1). The alignment was primarily based on the Ti/Sum ratio. We assume neither overlap nor hiatus between NYK4 and NYK5. As previously described, the TDV core sections were sampled without overlap, in a continuous sequence, and therefore do not need to be correlated.

For establishing the chronologies of the composite cores, the Bacon package (v. 2.5.0, Blaauw and Christen, 2013) with the IntCal20 dataset (Reimer et al., 2020) were used in R (v. 4.0.3, Core, 2015). The age-depth models were constructed using a mean accumulation rate (acc.mean) of 20 yr/mm for both cores and upper (d.min) and lower (d.max) depths set to the upper- and lowermost depths of the cores. For >5 cm thick tephra layers (Saksunarvatn in TDV and V1477 in NYK), a slump was added to reflect the increased sedimentation rate at deposition.

3.6 DNA extraction and amplification

DNA analyses were performed in the ancient DNA laboratory at the Arctic University Museum, Tromsø. Initially, 8-10 g of sediments were homogenised. DNA was extracted from

subsamples of ~0.3 g using PowerSoil Power Lyser kit and incorporating a bead beating step as in Alsos et al. (2020). We included negative controls during sampling from the core, extraction, and PCR setup, as well as positive controls during PCR. In total, 146 samples, 14 sampling and extraction negative controls, 4 PCR negative and 4 PCR positive controls were analysed.

We amplified the short and variable P6 loop region of the chloroplast trnL (UAA) intron (Taberlet et al., 2007), following the same analysis protocol Alsos et al. (2020), and running 8 PCR replicates on each DNA extract using unique 8 or 9 bp long tags added to the 5' end of each primer. We pooled the PCR replicates, and thereafter cleaned and quantified them using Qubit (Invitrogen™ Quant-iT™ and Qubit™ dsDNA HS Assay Kit, Thermofisher). We converted the pools into DNA libraries using a Truseq DNA PCR-free low-throughout library prep kit (Illumina). The library was quantified by qPCR using the KAPA Library Quantification Kit for Illumina sequencing platforms (Roche) and a Quantstudio 3 (Life Technologies). The library was normalised to a working concentration of 10 nM using the molarity calculated from qPCR adjusted for fragment size. Sequencing was conducted on an Illumina NextSeq 500 platform (2x150 bp, mid-output mode, dual indexing) at the Genomics Support Centre Tromsø (UiT).

3.7 DNA sequencing analyses and filtering

We aligned, filtered and trimmed the next-generation sequencing data using the OBITools software package (Boyer et al., 2016) and a custom R-script (available at https://github.com/Y-Lammers/MergeAndFilter). The new reference library PhyloNorway, consisting of 2051 specimens of 1899 vascular plant taxa from Norway and the Polar Regions

was used (Alsos et al., 2020). Additionally, we used the circumarctic/circumboreal ArcBorBryo library, containing 2445 sequences of 815 arctic and 835 boreal vascular plants as well as 455 bryophytes (Soininen et al., 2015; Sønstebø et al., 2010; Willerslev et al., 2014). Our third reference library was obtained by running the *ecotag* program on the EMBL (rl143) nucleotide reference database. We only retained sequences with 100% match to one of the reference libraries and a minimum of 3 replicates across the dataset. As 94% of the taxa in Iceland also are found in Norway (Alsos et al., 2015), match to PhyloNorway was given priority for vascular plants, whereas match to ArcBorBryo was given priority for bryophytes. For sequences assigned to several taxa, the most likely taxa with 100% match were listed based on known presence in the native flora.

We manually cross-checked that identifications were consistent among the reference libraries used, and inconsistent taxonomic assignments were cross-checked using NCBI BLAST. As this process is time-consuming, we only checked sequences that occurred with a minimum 10 replicates if they had 100% match to one of the regional reference libraries (PhyloNorway or ArcBorBryo). We followed the taxonomy of Wąsowicz (2020). Furthermore, the quality of each sample was assessed following the method described by Rijal et al. (2020).

3.8 Data analyses

Initial diagrams were plotted in R version 4.0.3 using the rioja (v0.9.26) and ggplot2 (v3.3.2) packages. We explored zonation for DNA using constrained incremental sum of squares (CONISS) as implemented in rioja. Final diagrams were constructed using Tilia v.2.6.1 (https://www.tiliait.com/).

4. Results

4.1 Chronology and core correlation

All radiocarbon ages, calibrated median ages and 2σ age intervals are presented in Table 1, and the tephra marker layers in Table 2. The identified tephra layers have been correlated to source volcanic system and particular volcanic event using geochemistry, stratigraphic position and age. Geochemical correlation of Hekla 1104, Hekla 3, Hekla 4 and Saksunarvatn ash in TDV and V1477, Hekla 3 and Hekla 4 in NYK are shown on elemental bi-plots in Supplementary Fig. S2. The complete geochemical dataset and standard runs are presented in Supplementary Table S1. Given the geochemical similarity of the Saksunarvatn/G10ka series tephra (Óladóttir et al., 2020) and the relatively short phase of associated volcanism compared to the Holocene scale of this study, we refer to the tephra horizon as a marker layer according to the Greenland ice core chronology (Rasmussen et al., 2006). Radiocarbon age Ua-65341 from NYK (Table 1) is an outlier when compared to Ua-67058 and tephra marker layers V1477 and Hekla 3 stratigraphically below, and was excluded when running the final age-depth model for NYK (Fig. 3B).

The TDV sections were sampled without an overlap, and stacked on top of each other to establish the composite record. The age-depth model supports this approach. The 915 cm long TDV record spans the last *c*. 12,000 years (Fig. 3A). The correlation of the NYK core sections showed large overlaps between NYK1, NYK2 and the upper half of NYK3 (Supplementary Fig. S1). Also, part of NYK3 and NYK4 were overlapping, whereas there was no overlap between NYK4 and NYK5. Presuming no hiatus between NYK4 and NYK5 resulted in a fairly linear age-depth model for that part of the record, and we therefore consider it a

382 reasonable assumption. The 464 cm long composite NYK record spans the last *c*. 8600 years
383 (Fig. 3B).
384
385
386 ## 4.2 Lithology and stratigraphy
387 Four main sedimentary facies were identified in Torfdalsvatn: clay, clayey gyttja, laminated
388 gyttja, and tephra (Fig. 4A; Supplementary Figs S3-S9). The clay facies is grey and
389 homogeneous, and the MS and Ti/(inc+coh) are high. We interpret this facies as clay formed
390 from suspension settling of particles originating from sediment-laden streams flowing into the
391 basin. The clayey gyttja is brown-grey and the MS and Ti/(inc+coh) records indicate a lower
392 minerogenic content than in the clay. We interpret this facies as formed by organic
393 sedimentation and inflow of minerogenic material by runoff from the catchment (e.g., (Björck
394 et al., 1992; Rundgren, 1995)). The laminated gyttja facies is light olive-brown and contains
395 numerous silt-sand sized tephra beds. The magnetic susceptibility (MS) and the Ti/(inc+coh)
396 are very low, indicating less inflow of minerogenic material compared to the clayey gyttja.
397 The tephra facies appear as 1-180 mm thick, black or white beds of silt-sand size volcanic
398 glass. Angular tephra grains and characteristic chemical composition suggest that they are not
399 reworked. Therefore, we interpret the tephra as originating from airborne material during
400 volcanic eruptions (e.g., Gudmundsdóttir et al., 2012; Larsen and Eiríksson, 2008; Lowe,
401 2011).
402
403 Three main sedimentary facies were identified in Nykurvatn (Fig. 4B; Supplementary Figs
404 S10-S14). The laminated gyttja facies is light olive-brown, containing silt-sand sized tephra
405 beds. It has an organic content of 1-11%, with the lowest values in the tephra and highest
406 values in the massive parts of the gyttja. As in Torfdalsvatn, we interpret the gyttja facies as

formed by organic sedimentation and inflow of minerogenic material by runoff. The tephra facies are 1-180 mm thick, black or white beds of silt-sand size. Again, we interpret it as originating from airborne material from volcanic eruptions (Gudmundsdóttir et al., 2012; Larsen and Eiríksson, 2008; Lowe, 2011). The grey-brown silt-sand facies appear as 3-5 cm thick beds and only occur in NYK5. We interpret this facies as deposited from higher input of minerogenic material to the basin e.g., by runoff and/or aeolian activity.

4.3 *sed*aDNA data

In total, 25,662,641 merged paired-end reads were obtained for both lakes. Out of these, 16,383,211 reads, belonging to 324 sequences were retained after filtering, where 147 sequences were identified with PhyloNorway, 191 with ArctBorBryo and 308 with EMBL (Supplementary Tables S2-3). Among sequences with less than 10 repeats across all samples, we discarded 64 that had <100% match to the local reference libraries. We assume these mainly represent homopolymer variants of more common sequences, PCR and sequencing artefacts, but it also excluded some taxa that were rare in our dataset (e.g., *Anthyrium*). The remaining 260 sequences were manually cross-checked for consistency. Sequences that were assigned to the same taxon and co-occurring in samples, were merged. Also, 402,835 reads of 40 sequences of known food contaminants or those that were biogeographically unlikely were omitted. We removed four samples from Torfdalsvatn (two of them from the Saksunarvatn tephra layer) and two samples from Nykurvatn due to low quality scores (Supplementary Table S4). This resulted in a final data set of 15,966,705 reads of 191 taxa (146 vascular plants and 45 bryophytes).

4.4 Vegetation at Torfdalsvatn

At Torfdalsvatn, we identified 60 taxa of forbs, 31 bryophytes, 23 graminoids, 11 woody, 16 aquatic macrophytes, 4 ferns, 3 horsetails, 1 club moss and 3 taxa of algae, in total 152 taxa (Fig. 5, Supplementary Table S4). The CONISS analyses identified 5 zones (TDV-DNA1 to TDV-DNA5) with breakpoints at approximate 10,100 cal. yr BP, 6700 cal. yr BP, 2400 cal. yr BP and 950 cal. yr BP.

The oldest CONISS zone (TDV-DNA1, 11,600-10,100 cal. yr BP) included the grey clay, the brown-grey clay, and the start of the light brown-olive gyttja (Fig. 4A). The grey clay was characterised by high arctic forbs (such as *Saxifraga* spp., *Ranunculus, Draba*), grasses (most likely dominated by *Phippisa algida*, but also *Trisetum* and *Alopecurus*) and diverse bryophytes (19 taxa, Fig. 5), with the bryophytes being most abundant (Fig. 6). During this period, the highest proportion of unidentified reads occurs, potentially representing algae which are generally poorly represented in reference libraries. This is also the period with the highest abundance of graminoids in this record, which constitutes up to 34% of the terrestrial plant reads (Fig. 6C, Supplementary data S5). Note however that graminoids may be underestimated with our DNA protocol (Alsos et al., 2018). The diversity increased in the brown-grey clay (from *c*. 10,850 cal. yr BP) with more high arctic forbs like *Oxyria digyna, Koenigia islandica, Cerastium, Micranthes* and *Cardamine polemoioides,* the first appearance of sedge (*Carex maritima*) and seven more bryophytes (Fig. 5). After that, the forbs, mainly *Saxifraga* spp., almost completely replaced the bryophytes for a short period (Fig. 6). Only after the transition to the light brown-olive gyttja (*c*. 10,400 cal. yr BP), the first woody species appear with the dwarf shrub *Empetrum nigrum* and the willow *Salix*, which most likely represent *Salix arctica* or *S. herbacea*. At the same time, 15 new forbs, eight new graminoids (including rushes such as *Luzula* spp.) and three new bryophytes appear. In

addition, the first aquatic macrophyte (*Myriophyllum alterniflorum*), fern (*Cystopteris fragilis*), algae (*Nannochloropsis gaditana*), and horsetails (*Equisetum* spp.) appear (Fig. 5).

No further change in lithology occurs in the other CONISS zones. Zone TDV-DNA2 (10,100-6700 cal. yr BP) was characterised by a massive immigration of species, with the arrival of *Betula* (either *B. nana* or *B. pubescens*), *Sorbus aucuparia, Juniperus communis* and the dwarf shrubs *Kalmia procumbens, Vaccinium uliginosum, V. myrtillus, Thymus praecox* and *Dryas octopetala* (Fig. 5). In total, 23 new taxa of forbs arrived, the majority of them appearing in most samples onwards, for example *Galium,* Asteraceae, *Alchemilla, Rumex* and *Plantago*, but also some rare forbs such as Orchidaceae. Also, a few new graminoids, ferns, algae, horsetails and one club moss arrive (Fig. 5). This zone is when most aquatic macrophytes arrive, making up >50% of the reads in most samples for the rest of the lake record (Fig. 6A). In addition to the massive immigration, this zone is characterised by the disappearance of many of the early high arctic forbs, *Phippsia*, and bryophytes.

The transition to zone TDV-DNA3 (6700-2400 cal. yr BP) is characterised by arrivals of a few new species. Rowan (*Sorbus aucuparia*) appears in almost every sample in the first two thirds of the zone but then it disappears *c.* 4000 cal. yr BP. The change is most clear in the aquatics, with the aquatic macrophyte *Littorella uniflora* and the algae *Cosmarium botrytis* appearing. Also, a few members of the rose family (*Potentilla anserina, Rubus/Fragaria*) appear. There is a sudden peak in the proportion of trees and shrubs at 4300 cal. yr BP (Fig. 6C), mainly caused by 40% *Juniperus communis* in a single sample (Supplementary Table S5); this may be due to occurrence of macrofossils in that sample rather than a change in the vegetation. There is no disappearance of taxa, but the fern *Gymnocarpium dryopteris* becomes less common.

TDV-DNA4 (2400-950 cal. yr BP) is poorly distinguished from the previous zone and mainly represents a change in abundance of some taxa, such as an increase in *Juniperus communis, Vaccinium myrtillus, Thymus praecox, Dryas octopetala, Festuca richardsonii, Juncus trifidus,* and *Thalictrum alpinum* (Supplementary Table S5). Only scattered records of one new aquatic macrophyte (*Hippuris vulgaris*), two graminoids, one bryophyte and one forb are observed (Fig. 5). However, some of the early high arctic taxa, such as *Silene acaulis* and *Oxyria digyna,* reappear. A reduction in a few taxa, such as *Equisetum variegatum* and *Lycopodium*, is also observed.

The uppermost zone, TDV-DNA5, starts at ~950 cal. yr BP (AD 1000, taken as midpoint between sample TDV.79 at median age 1055 cal. yr BP and TDV.80 at 846 cal. yr BP). According to the CONISS analyses, the change at 950 cal. yr BP represents the most pronounced change since the onset of the Holocene warming around 10,100 cal. yr BP (Fig. 5). Notably, *Juniperus communis* suddenly disappears after being found in almost every sample from 10,000 cal yr BP to 1055 cal. yr BP (AD 895). A whole range of forbs disappears or reduces in abundance after being common for nearly 9000 years: *Ranunculus confervoides, R. reptans, Angelica archangelica, A. sylvestris, Rhodiola rosea, Galium, Rhinanthus minor and Geum rivale.* In contrast, two of the high arctic forbs, *Koenigia islandica* and *Oxyria digyna*, become common again, together with arrivals of some new arctic-alpine forbs, e.g., *Saxifraga oppositifolia, Antennaria alpina*, and *Scorzoneroides autumnalis*. *Plantago maritima* increases in abundance. Notably, a sequence identified as potential archaeophyte (*Phleum pratense* and/or *Alopecurus pratensis*) appears. Three aquatic macrophytes, *Caltha palustris, Callitriche hermaphroditica* and *Potamogeton berchtoldii,*

disappear, indicating a shift in the lake water conditions. The proportion of trees and shrubs increases towards the end of this zone, mainly due to an increase in *Salix* (Figs 5-6).

4.5 Vegetation at Nykurvatn

We identified 66 taxa of forbs, 38 bryophytes, 27 graminoids, 15 aquatic macrophytes, 14 woody, 5 ferns, 3 horsetails, 1 club moss and 3 taxa of algae, in total 172 taxa (Fig. 7, Supplementary Table S4). CONISS analyses did not identify any significant zonation in the DNA data. This is in accordance with the uniform lithology (Fig. 4B). All the dominant taxa occurred already in the oldest few samples. Notably, the record starts at 8600 cal. yr BP, which is ~1500 years after the massive immigration observed at Torfdalsvatn. *Salix* was found in all samples, and *Betula* in all except two, both of which had generally low DNA quality scores. The non-native tall shrub/tree *Alnus* appeared in two samples (5200 and 200 cal. yr BP), whereas the native *Sobus aucuparia* only was found in one sample from 1200 cal. yr BP. *Juniperus communis* was common until 7000 cal. yr BP, after which it only had scattered occurrences, and it was not found in samples from the last 1000 years. Also, some arctic-alpines were most abundant in the early part and then again in the last 1000 years (e.g., *Euphrasia*, *Galium*, *Silene acaulis, Oxyria digyna, Antennaria alpina* and *Pedicularis flammea*). There is a change in aquatic macrophytes, with the more nutrient demanding species *Potamogeton berchtoldii* and *Caltha palustris* only being common from 7600-3300 cal. yr BP. In contrast to Torfdalsvatn, bryophytes were common throughout the core. One taxa classified as naturalised non-native taxon (Wąsowicz, 2020), *Lamium album* (four records 8100-2300 cal. yr BP), was also observed.

4.6 Richness and accumulation of species pool

The earliest recorded arrival date of each species is given in Supplementary Table S6. At both sites, there is a rapid increase of species in the early part of the cores. At Torfdalsvatn, there is a steep increase in species richness of bryophytes prior to the increase in forbs, whereas the opposite is observed for Nykurvatn (Fig. 8). At both sites, the richness of trees and shrubs, dwarf shrubs, vascular cryptogams, and aquatic macrophytes levelled off after the first wave of colonisation. The number of forb taxa continued to increase at both sites. The apparent levelling off during some shorter periods at Nykurvatn (e.g., ~6000, ~4000, 2500 and 1500 cal. yr BP) may represent sampling artefacts as it coincides with periods with less dense sampling interval (Fig. 7). In contrast, the levelling off at 5900-700 cal. yr BP at Torfdalsvatn is in a period with dense sampling (Fig. 5), so this is assumed to represent a real pattern. Note that the number of forbs increases again at Torfdalsvatn from around 600 cal. yr BP (1350 AD). The number of bryophytes levels off at 10,300 cal. yr BP at Torfdalsvatn, with only four additional bryophyte taxa thereafter. At Nykurvatn, the number of bryophytes continues to increase with a pronounced increase from 1200 cal. yr BP (750 AD). On the contrary, the number of graminoids levels off at 3800 cal. yr BP at Nykurvatn, whereas at Torfdalsvatn graminoids increases up to 8800 cal. yr BP and then again from 5000 cal. yr BP.

When data from both sites as well as the review study are aggregated, only 1-2 new taxa of vascular cryptogams, trees and shrubs, dwarf shrubs or aquatic macrophytes are observed after 8000 cal. yr BP (Fig. 8C). No new graminoids and only one new forb arrive after 4500 cal. yr BP, whereas bryophytes increase in the last 1000 years.

The average raw richness was 13.92 for Torfdalsvatn and 19.19 for Nykurvatn. The richness per sample levelled off from around 8000 cal. yr BP at Torfdalsvatn, whereas it showed an

556 almost linear increase of 3.5 taxa per millennium for Nykurvatn (Fig. 8D). The species pool at
557 Torfdalsvatn showed a steep increase from 11,600 to ~9000 cal. yr BP, and a continuous
558 increase after that (Fig. 8D). The initial increase at Nykurvatn was even steeper, and continues
559 to increase until present. The detected regional species pool based on both lakes and review of
560 earlier records shows a steep increase until around 8000 cal. yr BP, when >80% of the total
561 taxa had arrived, and hardly any new taxa after 4500 cal. yr BP (Fig. 8D).
562
563

564 ## 5. Discussion

565 Our records characterising Early Holocene vegetation and plant communities reflect summer
566 temperature conditions in accordance with previous Holocene Thermal Maximum
567 reconstructions (Caseldine et al., 2006; Eddudóttir et al., 2015; Hallsdóttir and Caseldine,
568 2005; Harning et al., 2018). Fig. 9 summarises key vegetation data from each site compared to
569 sea-ice proxy IP_{25} data from the North Iceland shelf (Cabedo-Sanz et al., 2016; Xiao et al.,
570 2017) and reconstructed mean summer air temperature anomalies from Northwest Iceland
571 (Harning et al., 2020). The largest changes in taxonomic composition and dominance were
572 observed at Torfdalsvatn at the onset of the Holocene warming around 10,100 cal. yr BP,
573 coinciding with peak summer insolation (Berger and Loutre, 1991), and at Landnám about
574 1000 years ago. The Nykurvatn record starts at 8600 cal. yr BP, and exhibits the largest shift
575 following Landnám, although without statistical significance. Furthermore, minor changes
576 were observed in both records, mainly in the aquatic macrophytes. While the taxonomic
577 composition was rather stable from 10,100-1000 cal. yr BP, the proportion of different plant
578 functional groups fluctuated. The majority of taxa immigrated before 8000 cal. yr BP, thus
579 prior to the Holocene Thermal Maximum (Geirsdóttir et al., 2020). The peak immigration was

around 10,000 cal. yr BP, when (Fig. 9), when occasional sea ice connected Iceland to northern Scandinavia and Russia (Alsos et al., 2016).

5.1 Possible glacial survival of high arctic species

The assemblage of high arctic taxa found in the oldest samples at Torfdalsvatn, suggests that these might have survived the LGM in Iceland. However, as we have no sediments older than *c.* 11,600 cal. yr BP, we have no direct proof of glacial survival. Glacial survival of high arctic forbs, graminoids and bryophytes is less controversial and has also been found in a LGM refugium in northern Norway (Alsos et al., 2020). In our current study, possible glacial survival taxa based on their occurrence in the three oldest samples are *Saxifraga cespitosa, Saxifraga cernua* and/or *rivularis* and *Phippsia algida*. For *S. cernua,* a considerable intermingling in the amphi-Atlantic region was inferred, whereas no genetic variation was detected within the region in *P. algida* (Aares et al., 2000; Brochmann et al., 2003; Bronken, 2001). We are not aware of any phylogeographical studies of *S. cespitosa* that include Iceland, but a study of populations in Svalbard and Norway concludes high dispersal potential (Brochmann et al., 2003; Tollefsrud et al., 1998). Notably, potential glacial survival has been suggested for *S. rivularis* in Svalbard, but not in Iceland, based on studies of AFLP fingerprinting (Westergaard et al., 2010). Thus, our new data neither prove nor disprove glacial survival.

5.2 Colonisation of plants

The initial steep increase in accumulated species richness at both sites represents an overestimation of colonisation at that time. For Torfdalsvatn, we know that many of the taxa were present earlier (Rundgren, 1998, 1995), and for Nykurvatn, our record does not include

605 the earliest vegetation in the region. Thus, numerous species arrived prior to their being
606 detected in our *sed*aDNA records (Figs 8-9). Also, it takes time from the first arrival of a
607 propagule to become spread around Iceland. Therefore, it is likely that the massive
608 immigration mainly took place prior to 10,100 cal. yr BP. Sea ice between Iceland and North
609 Norway was common to dense prior to 11,000 cal. yr BP (Alsos et al., 2016). In addition,
610 catastrophic draining of the Baltic Ice Lake around 11,700 cal. yr BP caused meltwater and
611 potentially ice loaded with sediments to drift into the Nordic Seas (Björck, 1995; Nesje et al.,
612 2004). Both sea ice and drift ice have already been identified as a major dispersal vector for
613 beetles to Iceland (Panagiotakopulu, 2014). After that, sea ice was only found occasionally
614 around Iceland 11,000-8000 cal. yr BP (Alsos et al., 2016), and may have been completely
615 absent on the North Iceland shelf 11,700-6800 cal. yr BP (Fig. 9, Xiao et al., 2017). This
616 direct evidence of a massive immigration prior to 10,100 cal. yr BP. supports that sea ice may
617 have acted as an important dispersal vector either by direct transport of diaspores or by a
618 combination of wind and sea ice (Alsos et al., 2016; Panagiotakopulu, 2014), although other
619 dispersal vectors as birds, wind and sea current also may have contributed (Alsos et al., 2015).
620
621 From around 8000 cal. yr BP, hardly any taxa of trees, shrubs, dwarf shrubs, aquatic
622 macrophytes or cryptogams were detected in the lake records. These are functional groups
623 that have rather few taxa in Iceland (Wąsowicz, 2020). There are, however, more taxa of these
624 groups in the assumed main source regions Scandinavia and the British Isles (Elven, 2005;
625 Stace, 1997). As aquatic macrophytes are well dispersed by birds and appeared within 1-3
626 decades after warming in western Norway (Birks, 2000), they may not be limited by
627 availability of sea ice. They may, however, be limited by nutrients and light availability or
628 other factors related to habitat diversity in Iceland. Trees, shrubs, dwarf shrubs, and

629 cryptogams on the other hand, might have been more limited by lack of sea ice in the Middle
630 Holocene.
631
632 In contrast, new taxa of forbs, graminoids, and bryophytes continued to be detected until 4500
633 cal. yr BP (bryophytes until present). Forb is the functional group with the highest number of
634 taxa in total (Fig. 8). The majority of forbs rely on insects for pollination. Thus, late
635 colonisation of forbs may be due to pollinator limitation. The arrival time for most pollinators
636 is not known (Panagiotakopulu, 2014). However, we note that most forb taxa and most
637 graminoids that are only recorded after 4500 cal. yr BP are found scattered in a few samples
638 and only in a few of the PCR repeats (Figs 5 and 8). As the ability to detect rare taxa in
639 *sed*aDNA is limited (Alsos et al., 2018), they may represent scattered records of taxa that
640 were also present earlier. Indeed, *Saxifraga oppositifolia* was recorded on Svalbard and
641 Greenland 11,000-10,000 cal. yr BP (Bennike et al., 1999; Bennike and Hedenäs, 1995), so it
642 is not unlikely that it was also present in Iceland at that time. The late arriving bryophytes
643 however, were detected in many samples and often all eight PCR repeats, suggesting that
644 these taxa are less likely to have been overlooked in earlier samples. Bryophytes have small
645 spores that in general are widely dispersed. Furthermore, they are important pioneers on
646 volcanic substrate, producing organic material for secondary colonisers (Ingimundardóttir et
647 al., 2014). While late arrival of some species cannot be excluded, the cooler conditions during
648 the Little Ice Age (AD 1250/1500-1900, Mann, 2002) may have made bryophytes more
649 abundant and thus more likely to be detected.
650
651 The overall accumulation of plant taxa in Iceland is greatest during the Late Glacial and Early
652 Holocene (>80% before 8000 cal. yr BP). Furthermore, these records from Iceland exhibit an
653 earlier accumulation compared to an accumulation curve for plant taxa based on *sed*aDNA

654 analyses of ten lakes in northern Fennoscandia (⅔ before 8000 cal. yr BP, Rijal et al., 2020).
655 This could be related either to species source pools or dispersal vectors. The flora in Iceland's
656 main source regions, Scandinavia (Elven, 2005) and the British Isles (Stace, 1997), are about
657 four times as large as the flora of Iceland (Alsos et al., 2015; Wąsowicz, 2020). While some
658 of these species require warmer conditions than currently found in Iceland, it is clear that
659 there is a large species pool that never made it across the ocean. Thus, we do not think that the
660 size of the source pool *sensu* (Harrison, 2020) has limited colonisation of plants in Iceland. As
661 our *sed*aDNA record is based on only two lakes, both lacking the basal sediments, the
662 difference between Iceland and northern Fennoscandia is likely underestimated. The
663 accelerated accumulation of taxa in Iceland compared to northern Fennoscandia may relate to
664 the disappearance of the main dispersal vector (sea ice) during the Middle Holocene, and
665 therefore we did not observe the same dispersal lag as in northern Fenoscandia (Rijal et al.,
666 2020).
667
668 Ultimately, if sea ice has been an important natural vector for plant dispersal to Iceland as our
669 data suggest, we may not expect a wave of immigration of new taxa to Iceland due to the
670 decreased ice cover following ongoing climate change. Furthermore, most modern sea ice
671 originates from the Arctic Ocean, and is transported south through the Denmark Strait by the
672 East Greenland Current. Anthropochore introduction, however, is assumed to increase unless
673 measures are taken (Wasowicz et al., 2013).
674

675 ### 5.3 Early Holocene vegetation development

676 The Saksunarvatn tephra layer provides a firm tie point between our TDV core and cores from
677 Torfdalsvatn previously investigated by Rundgren (1995) and Florian (2016), and magnetic
678 susceptibility provided additional alignment to the core by Florian (2016). As in the Rundgren

679 (1995) study, the Saksunarvatn tephra overlaid a layer of clayey gyttja, which again overlays
680 a layer of clay. We did not observe the Vedde tephra layer (12,100 cal. yr BP, Rasmussen et
681 al., 2006), thus TDV only extends down to somewhere in the clay layer (pollen zone T4-T5)
682 of Rundgren (1995).
683
684 The lowest part of our core (TDV-DNA1) is dominated by bryophytes with some *Saxifraga*,
685 which aligns with the T4 zone of low pollen concentrations detected by Rundgren (1995).
686 This is also the period with the highest proportion of unidentified sequences (Fig. 6). As the
687 majority of bryophytes and vascular plants known from Iceland are covered in our reference
688 library, the unidentified sequences likely reflect algae, which have limited reference material
689 available for the marker used. This aligns with assumed high autochthonous production of
690 algae based on algal pigments and a low ratio of total organic carbon to biogenic silica
691 (Florian, 2016).
692
693 In our core, the bryophytes are rapidly replaced by high proportions of *Saxifraga* species,
694 while graminoids remain common and peak around 10,800 cal. yr BP. This likely corresponds
695 to the increase in grass pollen exhibited in pollen zone T5 of Rundgren (1995). Thereafter,
696 both *sed*aDNA and pollen (T6) show an overall high number of taxa; such as *Salix, Empetrum*
697 *nigrum, Oxyria digyna, Koenigia islandica, Ranunculus,* Caryophyllaceae (identified to
698 *Cerastium alpinum/nigrescens* and *Silene acualis* in *sed*aDNA), and *Hornungia* type pollen
699 (identified to *Cardamine polemonioides* in *sed*aDNA)(Rundgren, 1998, 1995). This is a
700 period characterised by increasing ratios of carbon to nitrogen and total organic carbon to
701 biogenic silica (Florian, 2016), suggesting enhanced terrestrial production.
702

Our TDV-DNA2 (10,100-6700 cal. yr BP) is characterised by the appearance of *Juniperus communis*, which is assumed to correspond to pollen zone T8. In contrast to the previous record (Rundgren, 1998), we observed a massive immigration of new taxa at this transition, especially of forbs which are generally poorly represented in pollen. The transition to pollen zone T9 at around 8700 cal. yr BP is mainly quantitative, and could not easily be aligned with any change in the DNA data (falls within TDV-DNA2). Note that the two dates Rundgren has from T9 are reversed (7940+/-130 and 7860+/-120 BP). Also, there is a 4000 year hiatus in the record of Rundgren (1998), so his analyses stop here. Soon after, the first aquatic macrophytes appear in our DNA record, and they become the most dominant group in terms of DNA reads. This aligns with the increase in $\delta^{13}C$ just after deposition of the Saksunarvatn tephra layer, supporting an increase in organic production by aquatic macrophytes (Florian, 2016) consistent with a clearer water column following the reduced minerogenic influx also shown here by the MS profile (Fig 9A). The $\delta^{13}C$ remains higher than -20‰ until the last millennium (Florian, 2016), which agrees with the high proportion of DNA reads identified as aquatic macrophytes. The high proportion of aquatic macrophytes may also explain the lower richness detected at Torfdalsvatn compared to Nykurvatn, as the richness of terrestrial taxa may be underestimated when >50% of the DNA reads are originating from aquatic taxa (Rijal et al., 2020).

5.4. Vegetation development during Middle and Late Holocene

At Nykurvatn, no significant changes in vegetation composition were found for the entire period of 8600 years, suggesting a very stable flora. While we cannot distinguish *Betula nana* from *B. pubescens* based on the DNA region studied, the lack of other forest taxa (e.g., few ferns) and the scattered occurrence of *Juniperus communis* (<8 PCR repeats except around

728 8000-7000 cal. yr BP) suggest that forest never developed at this site. Thus, this was therefore
729 not affected by oscillations in *Juniperus communis* and *Betula* cover. This interpretation is
730 supported by pollen studies from the northwestern highland (416 m a.s.l), where sensitivity to
731 climate and tephra deposition is demonstrated by floral communities in which the
732 thermophilous (Iceland) *Betula pubescens* is prominent (Eddudóttir et al., 2016, 2017). The
733 variations in LOI and Ti/Sum are likely caused by the numerous silt-sand sized tephra beds as
734 well as input of minerogenic material from runoff and aeolian activity, rather than major
735 environmental change within this period.
736
737 The occurrence of the non-native tall shrub/tree *Alnus* at 5200 and 200 cal. yr BP is somewhat
738 unexpected, especially as these do not fall within a warm period (Geirsdóttir et al., 2020). It
739 may be difficult to distinguish small amounts of *sed*aDNA from background contamination
740 (Alsos et al., 2020). However, we have never recorded *Alnus* as contamination in our
741 laboratorium so far (Rijal et al., 2020). Also, the scattered occurrence of *Alnus* in some pollen
742 records (Verhoeven and Louwye, 2015) suggests that it might have occurred in Iceland in the
743 past.
744
745 At Torfdalsvatn, the transition to zone TDV-DNA3 (6700-2400 cal. yr BP) represents a minor
746 change in the terrestrial vegetation, but rowan appears from 6500-4100 cal. yr BP. Rowan
747 also appears in pollen diagrams from northern and southern Iceland from ~6000 and 4500 cal.
748 yr BP (Eddudóttir et al., 2015; Hallsdóttir, 1995; Hallsdóttir and Caseldine, 2005). This tree
749 species has a slightly more southern distribution than *Betula pubescens.* It is believed that its
750 distribution is not limited by summer temperature *per se*, but rather by a combination of poor
751 drought tolerance, adaptation to short growing seasons and cold requirement for bud burst
752 (Raspe et al., 2000). This suggests that the winters were colder during this period, which

753 agrees with the re-occurrence of sea ice at the North Iceland shelf after *c*. 6800 cal. yr BP as
754 indicated by IP_{25} biomarker data (Xiao et al., 2017), and by the presence of quartz in marine
755 sediment cores after *c*. 7000 cal. yr BP (Andrews et al., 2009). The disappearance of rowan
756 around 4100 cal. yr BP is during a period with widespread ice cap expansion, decreasing
757 biogenic silica and increased landscape instability (Geirsdóttir et al., 2020).
758
759 There was a clear change in the aquatic flora of Torfdalsvatn with the aquatic macrophyte
760 *Littorella uniflora* appearing from 6800 cal. yr BP. This is approximately the same time as
761 $\delta^{15}N$ increases, $\delta^{13}C$ decreases, and there is a shift in algal pigments (Florian, 2016), possibly
762 related to lacustrine environmental changes. *Littorella uniflora* is rare in Iceland and not
763 detected in Skagi today (Kristinsson, 2010) although its occurrence in the top samples
764 suggests it is overlooked.
765
766 The change in abundance of some taxa at the transition to TDV-DNA4 (2400 cal. yr BP) with
767 scattered reappearance of some of the early high arctic taxa, such as *Silene acaulis* and *Oxyria*
768 *digyna,* may be a result of the stepwise cooling that started in Iceland around 5000 cal. yr BP,
769 with increased cooling around 2400 cal. yr BP (Geirsdóttir et al., 2020, 2019; Harning et al.,
770 2020). A similar change was also observed at Nykurvatn, where *Oxyria digyna* and *Silene*
771 *acaualis* increased from ~2000 cal. yr BP, and several arctic-alpines re-appeared.
772
773
774 ### 5.5 Landnám, Medieval Climate Optimum and Little Ice Age
775 The clearest indication we observed of human impact was the sudden disappearance of
776 *Juniperus communis* 1055 cal. yr BP (895 AD) at Torfdalsvatn and 910 cal. yr BP (1040 AD)
777 at Nykurvatn. Some grazing may favour this species and it is therefore commonly taken as a

778 grazing indicator, especially of dry pastures (Vorren, 1986), although grazing reduces
779 seedling survival (Thomas et al., 2007). The disappearance from the DNA record suggests
780 that in addition to grazing, it was cut. This is a species that was used as fuel, fodder for sheep
781 and as raw material for ropes and tools (Larsen and Others, 1990). A reduction in *Juniperus*
782 *communis* has also been observed in pollen records from *c*. 1000 cal. yr BP (Eddudóttir et al.,
783 2020, 2016). Additional indicators of Landnám were the increase in a few grass taxa at
784 Nykurvatn, as well as the reduction in *A. sylvestris* and disappearance of *Angelica*
785 *archangelica* at Torfdalsvatn. These are taxa that are known to be grazing sensitive and also
786 decrease or disappear in pollen records (Eddudóttir et al., 2020; Erlendsson, 2007). The latter
787 was also observed at Nykurvatn, but continued to grow there during the last 1000 years,
788 probably because this is a higher altitude site less influenced by human land use. While the
789 onset of the Medieval Climate Optimum coincides with Landnám, we did not see any strong
790 indication of more thermophilic flora. Thus, the change at around 950 cal. yr BP at both sites
791 (but only significant at Torfdalsvatn), is interpreted as mainly due to human impact.
792
793 The increase of high arctic taxa such as *Oxyria digyna, Koenigia islandica, Epilobium*
794 *anagallidifolium, Silene acaulis,* and *Dryas octopetala* at Torfdalsvatn and increase in
795 bryophytes at Nykurvatn occur during the Little Ice Age. Thus, in addition to the impact of
796 human land use, we see a clear effect of climate deterioration. This coincides with low
797 summer air temperatures and increased sea-ice cover on the North Icelandic shelf (Fig. 9;
798 Cabedo-Sanz et al., 2016; Miles et al., 2020).
799
800

6. Conclusions

By using *sed*aDNA, we obtained detailed records of arrival of species and the vegetation history at one lowland and one higher-altitude lake in Iceland. Our records confirm the presence of a high arctic vegetation prior to peak Holocene warming. Moreover, the high taxonomic resolution of these records allows for the estimation of arrival time. Over 80% of the recorded taxa had arrived by 8000 cal. yr BP, prior to the Holocene Thermal Maximum in Iceland. The main immigration event coincides with a period of more extensive sea ice, supporting the hypothesis that sea ice was an important dispersal vector to Iceland. To further improve estimates of arrival time, more sites should be investigated across the island, focusing especially on records that span the Late Glacial/Holocene transition. We found that the taxonomic composition of the flora was remarkably stable until Landnám, when some land-use intolerant taxa gave way rapidly. While ongoing global warming will allow more species to thrive in the Icelandic environment, natural colonisation may be limited by reduction in sea ice resulting in a shift to anthropochore dominated dispersal.

Acknowledgements

We would like to thank Lasse Topstad and Luca Elliott for help with DNA extraction, Dilli P. Rijal for help with R script for data analyses, and Ellen Elverland for help with identifying macrofossils. Claus Falkenberg Thomsen kindly assisted during fieldwork at Nykurvatn. Þorsteinn Jónsson and Höskuldur Þorbjarnarson assisted with coring at Torfdalsvatn. Kurt H. Kjær and Marie-Louise Siggaard-Andersen, GLOBE Institute, kindly contributed with ITRAX sediment core scanning. Bioinformatic analyses were performed on resources provided by UNINETT Sigma2 - the National Infrastructure for High Performance Computing and Data Storage in Norway. This project has received funding from the European Research Council (ERC) under the European Union's Horizon 2020 research and innovation

826 programme (grant agreement No 819192 to Alsos), from the Arctic Research and Studies
827 Program of the Ministries for Foreign Affairs of Norway and Iceland (grant agreement No.
828 2017-ARS-79772 to Schomacker), the Icelandic Research Fund (grant no. 141842-051;
829 Guðrún Gísladóttir), Landsvirkjun Energy Research Fund and the University of Iceland
830 Research Fund.

831

832 Author contributions

833 Project idea IGA and AS; acquiring funding IGA, AS, EE, GG, ÍÖB, SB, WRF; coring SB,
834 ÍÖB, EE, GG, SDE, WRF, AS; core sampling EMB, AR; lithology SEK, EMB, AR, AS;
835 identification of plant macrofossils for radiocarbon dating EMB, SEK, AS; analyses of tephra
836 EMB, ERG, WRF; age-depth modelling EMB, SEK, AS; DNA analyses MKFM and IGA;
837 data analyses IGA and YL; manuscript draft IGA, AS, YL and SEK. All co-authors
838 commented on the manuscript.

839

840 Declaration of competing interests

841 No competing interest to declare.

842

843 Data availability

844 Raw sequence read data will be uploaded on Dryad (XXXX). The data obtained after filtering
845 are given in Supplementary data Table 4-5.

846

847 Supplementary data

848 **Supplementary Table S1.** Results from major element analyses on identified tephra layers
849 and standard runs.

Supplementary Table S2. The number of unique barcodes and reads present in the data after each bioinformatic step.

Supplementary Table S3. Sequence identification with comments.

Supplementary Table S4. Final *sed*aDNA dataset for Torfdalsvatn (TDV) and Nykurvatn (NYK) given as the weighted number of PCR repeats.

Supplementary Table S5. DNA raw and filtered reads, technical and ecological quality scores and proportion of reads for functional groups and key species for Torfdalsvatn (TDV) and Nykurvatn (NYK).

Supplementary Table S6. First arrival of taxa based on the current study and previous review of all macrofossil and pollen studies (Alsos et al., 2016).

Supplementary Figures S1-S14

References

Aares, E., Nurminiemi, M., Brochmann, C., 2000. Incongruent phylogeographies in spite of similar morphology, ecology, and distribution: *Phippsia algida* and *P. concinna* (Poaceae) in the North Atlantic region. Plant Syst. Evol. 220, 241–261.

Alsos, I.G., Ehrich, D., Eidesen, P.B., Solstad, H., Westergaard, K.B., Schönswetter, P., Tribsch, A., Birkeland, S., Elven, R., Brochmann, C., 2015. Long-distance plant dispersal to North Atlantic

islands: colonization routes and founder effect. AoB Plants 7. https://doi.org/10.1093/aobpla/plv036

Alsos, I.G., Ehrich, D., Seidenkrantz, M.-S., Bennike, O., Kirchhefer, A.J., Geirsdottir, A., 2016. The role of sea ice for vascular plant dispersal in the Arctic. Biol. Lett. 12. https://doi.org/10.1098/rsbl.2016.0264

Alsos, I.G., Eidesen, P.B., Ehrich, D., Skrede, I., Westergaard, K., Jacobsen, G.H., Landvik, J.Y., Taberlet, P., Brochmann, C., 2007. Frequent long-distance colonization in the changing Arctic. Science 316, 1606–1609.

Alsos, I.G., Lammers, Y., Yoccoz, N.G., Jørgensen, T., Sjögren, P., Gielly, L., Edwards, M.E., 2018. Plant DNA metabarcoding of lake sediments: How does it represent the contemporary vegetation. PLoS One 13, e0195403.

Alsos, I.G., Sjögren, P., Brown, A.G., Gielly, L., Merkel, M.K.F., Paus, A., Lammers, Y., Edwards, M.E., Alm, T., Leng, M., Goslar, T., Langdon, C.T., Bakke, J., van der Bilt, W.G.M., 2020. Last Glacial Maximum environmental conditions at Andøya, northern Norway; evidence for a northern ice-edge ecological "hotspot." Quat. Sci. Rev. 239, 106364.

Andrews, J.T., Darby, D., Eberle, D., Jennings, A.E., Moros, M., Ogilvie, A., 2009. A robust, multisite Holocene history of drift ice off northern Iceland: implications for North Atlantic climate. Holocene 19, 71–77.

Axford, Y., Miller, G.H., Geirsdóttir, Á., Langdon, P.G., 2007. Holocene temperature history of northern Iceland inferred from subfossil midges. Quat. Sci. Rev. 26, 3344–3358.

Benediktsson, J., 1968. Islensk fornrit I. Íslendingabók – Landnámabók. Hið íslenska fornleifafélag, Reykjavik.

Bennike, O., Björck, S., Böcher, J., Hansen, L., Heinemeier, J., Wohlfarth, B., 1999. Early holocene plant and animal remains from North-east Greenland. J. Biogeogr. 26, 667–677.

Bennike, O., Hedenäs, L., 1995. Early Holocene land floras and faunas from Edgeøya, Eastern Svalbard. Polar Res. 14, 205–214.

Berger, A., Loutre, M.F., 1991. Insolation values for the climate of the last 10 million years. Quat. Sci. Rev. 10, 297–317.

903 Birks, H.H., 2000. Aquatic macrophyte vegetation development in Kråkenes Lake, western Norway,
904 during the late-glacial and early-Holocene. J. Paleolimnol. 23, 7–19.
905 Björck, S., 1995. A review of the history of the Baltic Sea, 13.0-8.0 ka BP. Quat. Int. 27, 19–40.
906 Björck, S., Ingólfsson, Ó., Haflidason, H., Hallsdöttir, M., Anderson, N.J., 1992. Lake Torfadalsvatn:
907 a high resolution record of the North Atlantic ash zone I and the last glacial-interglacial
908 environmental changes in Iceland. Boreas 21, 15–22.
909 Bjorkman, A.D., Myers-Smith, I.H., Elmendorf, S.C., Normand, S., Rüger, N., Beck, P.S.A., Blach-
910 Overgaard, A., Blok, D., Cornelissen, J.H.C., Forbes, B.C., Georges, D., Goetz, S.J., Guay, K.C.,
911 Henry, G.H.R., HilleRisLambers, J., Hollister, R.D., Karger, D.N., Kattge, J., Manning, P.,
912 Prevéy, J.S., Rixen, C., Schaepman-Strub, G., Thomas, H.J.D., Vellend, M., Wilmking, M., Wipf,
913 S., Carbognani, M., Hermanutz, L., Lévesque, E., Molau, U., Petraglia, A., Soudzilovskaia, N.A.,
914 Spasojevic, M.J., Tomaselli, M., Vowles, T., Alatalo, J.M., Alexander, H.D., Anadon-Rosell, A.,
915 Angers-Blondin, S., Beest, M. te, Berner, L., Björk, R.G., Buchwal, A., Buras, A., Christie, K.,
916 Cooper, E.J., Dullinger, S., Elberling, B., Eskelinen, A., Frei, E.R., Grau, O., Grogan, P.,
917 Hallinger, M., Harper, K.A., Heijmans, M.M.P.D., Hudson, J., Hülber, K., Iturrate-Garcia, M.,
918 Iversen, C.M., Jaroszynska, F., Johnstone, J.F., Jørgensen, R.H., Kaarlejärvi, E., Klady, R.,
919 Kuleza, S., Kulonen, A., Lamarque, L.J., Lantz, T., Little, C.J., Speed, J.D.M., Michelsen, A.,
920 Milbau, A., Nabe-Nielsen, J., Nielsen, S.S., Ninot, J.M., Oberbauer, S.F., Olofsson, J.,
921 Onipchenko, V.G., Rumpf, S.B., Semenchuk, P., Shetti, R., Collier, L.S., Street, L.E., Suding,
922 K.N., Tape, K.D., Trant, A., Treier, U.A., Tremblay, J.-P., Tremblay, M., Venn, S., Weijers, S.,
923 Zamin, T., Boulanger-Lapointe, N., Gould, W.A., Hik, D.S., Hofgaard, A., Jónsdóttir, I.S.,
924 Jorgenson, J., Klein, J., Magnusson, B., Tweedie, C., Wookey, P.A., Bahn, M., Blonder, B., van
925 Bodegom, P.M., Bond-Lamberty, B., Campetella, G., Cerabolini, B.E.L., Chapin, F.S., Cornwell,
926 W.K., Craine, J., Dainese, M., de Vries, F.T., Díaz, S., Enquist, B.J., Green, W., Milla, R.,
927 Niinemets, Ü., Onoda, Y., Ordoñez, J.C., Ozinga, W.A., Penuelas, J., Poorter, H., Poschlod, P.,
928 Reich, P.B., Sandel, B., Schamp, B., Sheremetev, S., Weiher, E., 2018. Plant functional trait
929 change across a warming tundra biome. Nature 562, 57–62.
930 Blaauw, M., Christen, J.A., 2013. Bacon Manual v2. 3.3.

931 Boyer, F., Mercier, C., Bonin, A., Le Bras, Y., Taberlet, P., Coissac, E., 2016. OBITOOLS: a unix-
932 inspired software package for DNA metabarcoding. Mol. Ecol. Resour. 16, 176–182.
933 Brochmann, C., Gabrielsen, T.M., Nordal, I., Landvik, J.Y., Elven, R., 2003. Glacial survival or *tabula*
934 *rasa*? The history of North Atlantic biota revisited. Taxon 52, 417–450.
935 Bronken, P., 2001. Circumpolar chloroplast and nuclear DNA variation in *Saxifraga cernua*.
936 University of Oslo, Oslo.
937 Bronk Ramsey, C., 2009. Bayesian analysis of radiocarbon dates. Radiocarbon 51, 337–360.
938 Cabedo-Sanz, P., Belt, S.T., Jennings, A.E., Andrews, J.T., Geirsdóttir, Á., 2016. Variability in drift
939 ice export from the Arctic Ocean to the North Icelandic Shelf over the last 8000 years: A multi-
940 proxy evaluation. Quat. Sci. Rev. 146, 99–115.
941 CAFF, 2013. Arctic Biodiversity Assessment: The full scientific report. CAFF - Conservation of
942 Arctic Flora and Fauna, Akureyri, Iceland.
943 Caseldine, C., Langdon, P., Holmes, N., 2006. Early Holocene climate variability and the timing and
944 extent of the Holocene thermal maximum (HTM) in northern Iceland. Quat. Sci. Rev. 25, 2314–
945 2331.
946 Clarke, C.L., Alsos, I.G., Edwards, M.E., Paus, A., Gielly, L., Haflidason, H., Mangerud, J., Hughes,
947 P.D.M., Svendsen, J.I., Bjune, A.E., 2020. A 24,000-year ancient DNA and pollen record from
948 the Polar Urals reveals temporal dynamics of arctic and boreal plant communities.
949 Core, R., 2015. Team. R: a language and environment for statistical computing.
950 Croudace, I.W., Rindby, A., Guy Rothwell, R., 2006. ITRAX: description and evaluation of a new
951 multi-function X-ray core scanner. Geological Society, London, Special Publications.
952 https://doi.org/10.1144/gsl.sp.2006.267.01.04
953 Dugmore, A.J., Cook, G.T., Shore, J.S., Newton, A.J., Edwards, K.J., Larsen, G., 1995. Radiocarbon
954 Dating Tephra Layers in Britain and Iceland. Radiocarbon.
955 https://doi.org/10.1017/s003382220003085x
956 Eddudóttir, S.D., Erlendsson, E., Gísladóttir, G., 2020. Landscape change in the Icelandic highland: A
957 long-term record of the impacts of land use, climate and volcanism. Quat. Sci. Rev. 240, 106363.
958 Eddudóttir, S.D., Erlendsson, E., Gísladóttir, G., 2015. Life on the periphery is tough: Vegetation in

959 Northwest Iceland and its responses to early-Holocene warmth and later climate fluctuations.
960 Holocene 25, 1437–1453.
961 Eddudóttir, S.D., Erlendsson, E., Tinganelli, L., Gísladóttir, G., 2016. Climate change and human
962 impact in a sensitive ecosystem: the Holocene environment of the Northwest Icelandic highland
963 margin. Boreas. https://doi.org/10.1111/bor.12184
964 Eidesen, P.B., Ehrich, D., Bakkestuen, V., Alsos, I.G., Gilg, O., Taberlet, P., Brochmann, C., 2013.
965 Genetic roadmap of the Arctic: plant dispersal highways, traffic barriers and capitals of diversity.
966 New Phytol. 200, 898–910.
967 Elven, R., 2005. Norsk Flora (= Lids Flora).
968 Erlendsson, E., 2007. Environmental change around the time of the Norse settlement of Iceland.
969 University of Aberdeen.
970 Felde, V.A., Grytnes, J.-A., Bjune, A.E., Peglar, S.M., Birks, H.J.B., 2018. Are diversity trends in
971 western Scandinavia influenced by post-glacial dispersal limitation? J. Veg. Sci. 29, 360–370.
972 Florian, C.R., 2016. Multi-Proxy reconstructions of Holocene environmental change and catchment
973 biogeochemistry using algal pigments and stable isotopes preserved in lake sediment from Baffin
974 Island and Iceland (PhD). University of England.
975 Forwick, M., 2013. How to use XRF core scanner data acquired with the Avaatech XRF core scanner
976 at the Department of Geology, University of Tromsø. A short manual. University of Tromsø,
977 Department of Geology.
978 Geirsdóttir, Á., Harning, D.J., Miller, G.H., Andrews, J.T., Zhong, Y., Caseldine, C., 2020. Holocene
979 history of landscape instability in Iceland: Can we deconvolve the impacts of climate, volcanism
980 and human activity? Quat. Sci. Rev. 249, 106633.
981 Geirsdóttir, Á., Miller, G.H., Andrews, J.T., Harning, D.J., Anderson, L.S., Florian, C., Larsen, D.J.,
982 Thordarson, T., 2019. The onset of neoglaciation in Iceland and the 4.2 ka event. Clim. Past 15,
983 25–40.
984 Giesecke, T., Wolters, S., Jahns, S., Brande, A., 2012. Exploring holocene changes in palynological
985 richness in northern Europe--did postglacial immigration matter? PLoS One 7, e51624.
986 Giesecke, T., Wolters, S., van Leeuwen, J.F.N., van der Knaap, P.W.O., Leydet, M., Brewer, S., 2019.

Postglacial change of the floristic diversity gradient in Europe. Nat. Commun. 10, 5422.

Graae, B.J., Pagh, S., Bruun, H.H., 2004. An experimental evaluation of the arctic fox (*Alopex lagopus*) as a seed disperser. Arct. Antarct. Alp. Res. 36, 468–473.

Gudmundsdóttir, E.R., Larsen, G., Eiríksson, J., 2012. Tephra stratigraphy on the North Icelandic shelf: extending tephrochronology into marine sediments off North Iceland. Boreas 41, 719–734.

Hallsdóttir, M., 1995. On the pre-settlement history of Icelandic vegetation (PhD thesis). University of Lund.

Hallsdóttir, M., 1987. Pollen analytical studies of human influence on vegetation in relatin to the landnám tephra layer in Southwest Iceland.

Hallsdóttir, M., Caseldine, C., 2005. The Holocene vegetation history of Iceland, state-of-the-art and future research, in: Caseldine, C., Russell, A., Hardardóttir, J., Knudsen, O. (Eds.), Modern Processes and Past Environments. Elsvier, Amsterdam.

Harning, D.J., Curtin, L., Geirsdóttir, Á., D'Andrea, W.J., Miller, G.H., Sepúlveda, J., 2020. Lipid biomarkers quantify Holocene summer temperature and ice cap sensitivity in Icelandic lakes. Geophys. Res. Lett. 47. https://doi.org/10.1029/2019gl085728

Harning, D.J., Geirsdóttir, Á., Miller, G.H., 2018. Punctuated Holocene climate of Vestfirðir, Iceland, linked to internal/external variables and oceanographic conditions. Quat. Sci. Rev. 189, 31–42.

Harrison, S., 2020. Plant community diversity will decline more than increase under climatic warming. Philos. Trans. R. Soc. Lond. B Biol. Sci. 375, 20190106.

Harter, D.E.V., Irl, S.D.H., Seo, B., Steinbauer, M.J., Gillespie, R., Triantis, K.A., Fernández-Palacios, J.-M., Beierkuhnlein, C., 2015. Impacts of global climate change on the floras of oceanic islands – Projections, implications and current knowledge. Perspect. Plant Ecol. Evol. Syst. 17, 160–183.

Heiri, O., Lotter, A.F., Lemcke, G., 2001. Loss on ignition as a method for estimating organic and carbonate content in sediments: reproducibility and comparability of results. J. Paleolimnol. 25, 101–110.

Icelandic Meteorological Office [WWW Document], 2020a. URL https://www.vedur.is/Medaltalstoflur-txt/Hraun_352_med6190.txt (accessed 8 of December 2020).

1015 Icelandic Meteorological Office [WWW Document], 2020b. URL
1016 https://www.vedur.is/Medaltalstoflur-txt/Stod_527_Skjaldtingsstadir.ArsMedal.txt (accessed 9 of
1017 December 2020).
1018 Ingimundardóttir, G.V., Weibull, H., Cronberg, N., 2014. Bryophyte colonization history of the virgin
1019 volcanic island Surtsey, Iceland. Biogeosciences 11, 4415–4427.
1020 Islandicum), D.I. (diplomatarium, 1857-1986. Íslenzkt fornbréfasafn III. Íslenzka bókmenntafélagið,
1021 Kaupmannahöfn (Copenhagen).
1022 Johansen, S., Hytteborn, H., 2001. A contribution to the discussion of biota dispersal with drift ice and
1023 driftwood in the North Atlantic. J. Biogeogr. 28, 105–115.
1024 Kristinsson, H., 2010. A guide to the flowering plants and ferns of Iceland, 3rd ed. Mál og menning,
1025 Reykjavik.
1026 Kylander, M.E., Ampel, L., Wohlfarth, B., 2011. High-resolution X-ray fluorescence core scanning
1027 analysis of Les Echets (France) sedimentary sequence: new insights from chemical proxies. J.
1028 Quat. Sci.
1029 Langdon, P.G., Leng, M.J., Holmes, N., Caseldine, C.J., 2010. Lacustrine evidence of early-Holocene
1030 environmental change in northern Iceland: a multiproxy palaeoecology and stable isotope study.
1031 Holocene 20, 205–214.
1032 Larsen, A.-C., Others, 1990. Norsemen's use of juniper in Viking Age Faroe Islands. Norsemen's use
1033 of juniper in Viking Age Faroe Islands. 61, 54–59.
1034 Larsen, G., Eiríksson, J., 2008. Late Quaternary terrestrial tephrochronology of Iceland—frequency of
1035 explosive eruptions, type and volume of tephra deposits. Journal of Quaternary Science.
1036 https://doi.org/10.1002/jqs.1129
1037 Larsen, G., Eiríksson, J., Knudsen, K.L., Heinemeier, J., 2002. Correlation of late Holocene terrestrial
1038 and marine tephra markers, north Iceland: implications for reservoir age changes. Polar Res. 21,
1039 283–290.
1040 Liu, S., Stoof-Leichsenring, K.R., Kruse, S., Pestryakova, L.A., Herzschuh, U., 2020. Holocene
1041 vegetation and plant diversity changes in the north-eastern Siberian treeline region from pollen
1042 and sedimentary ancient DNA. Frontiers in Ecology and Evolution 8, 304.

1043 Löve, A., Löve, D., 1963. North Atlantic biota and their History : a symposium held at the University
1044 of Iceland, Reykjavík, July 1962 under the auspices of the University of Iceland and the Museum
1045 of Natural History. Pergamon, Oxford.
1046 Lowe, D.J., 2011. Tephrochronology and its application: A review. Quat. Geochronol. 6, 107–153.
1047 Magnússon, Á., Vídalín, P., 1927. Jarðabók Árna Magnússonar og Páls Vídalín XIII. Hið íslenska
1048 fræðafélag, Copenhagen.
1049 Mann, M.E., 2002. Little ice age. Encyclopedia of global environmental change 1, 504–509.
1050 Miles, M.W., Andresen, C.S., Dylmer, C.V., 2020. Evidence for extreme export of Arctic sea ice
1051 leading the abrupt onset of the Little Ice Age. Sci Adv 6. https://doi.org/10.1126/sciadv.aba4320
1052 Möckel, S.C., Erlendsson, E., Gísladóttir, G., 2017. Holocene environmental change and development
1053 of the nutrient budget of histosols in North Iceland. Plant Soil 418, 437–457.
1054 National Land Survey of Iceland [WWW Document], 2020. . Lýsigagnagátt. URL
1055 https://gatt.lmi.is/geonetwork/srv/eng/catalog.search#/home (accessed 12.12.20).
1056 Nesje, A., Dahl, S.O., Bakke, J., 2004. Were abrupt Lateglacial and early-Holocene climatic changes
1057 in northwest Europe linked to freshwater outbursts to the North Atlantic and Arctic Oceans?
1058 Holocene 14, 299–310.
1059 Norðdahl, H., Ingólfsson, Ó., 2015. Collapse of the Icelandic ice sheet controlled by sea-level rise?
1060 arktos. https://doi.org/10.1007/s41063-015-0020-x
1061 Óladóttir, B.A., Thordarson, T., Geirsdóttir, Á., Jóhannsdóttir, G.E., Mangerud, J., 2020. The
1062 Saksunarvatn Ash and the G10ka series tephra. Review and current state of knowledge. Quat.
1063 Geochronol. 56, 101041.
1064 Paillard, D., Labeyrie, L.D., Yiou, P., 1996. AnalySeries 1.0: a Macintosh software for the analysis of
1065 geophysical time-series. EOS.
1066 Panagiotakopulu, E., 2014. Hitchhiking across the North Atlantic – Insect immigrants, origins,
1067 introductions and extinctions. Quat. Int. 341, 59–68.
1068 Patton, H., Hubbard, A., Andreassen, K., Auriac, A., Whitehouse, P.L., Stroeven, A.P., Shackleton, C.,
1069 Winsborrow, M., Heyman, J., Hall, A.M., 2017. Deglaciation of the Eurasian ice sheet complex.
1070 Quat. Sci. Rev. 169, 148–172.

1071 Rasmussen, S.O., Andersen, K.K., Svensson, A.M., Steffensen, J.P., Vinther, B.M., Clausen, H.B.,
1072 Siggaard-Andersen, M.-L., Johnsen, S.J., Larsen, L.B., Dahl-Jensen, D., Bigler, M.,
1073 Röthlisberger, R., Fischer, H., Goto-Azuma, K., Hansson, M.E., Ruth, U., 2006. A new
1074 Greenland ice core chronology for the last glacial termination. J. Geophys. Res. 111.
1075 https://doi.org/10.1029/2005jd006079
1076 Raspe, O., Findlay, C., Jacquemart, A.-L., 2000. Sorbus aucuparia L. J. Ecol. 88, 910–930.
1077 Reimer, P.J., Austin, W.E.N., Bard, E., Bayliss, A., Blackwell, P.G., Ramsey, C.B., Butzin, M.,
1078 Cheng, H., Lawrence Edwards, R., Friedrich, M., Grootes, P.M., Guilderson, T.P., Hajdas, I.,
1079 Heaton, T.J., Hogg, A.G., Hughen, K.A., Kromer, B., Manning, S.W., Muscheler, R., Palmer,
1080 J.G., Pearson, C., van der Plicht, J., Reimer, R.W., Richards, D.A., Marian Scott, E., Southon,
1081 J.R., Turney, C.S.M., Wacker, L., Adolphi, F., Büntgen, U., Capano, M., Fahrni, S.M.,
1082 Fogtmann-Schulz, A., Friedrich, R., Köhler, P., Kudsk, S., Miyake, F., Olsen, J., Reinig, F.,
1083 Sakamoto, M., Sookdeo, A., Talamo, S., 2020. The IntCal20 Northern Hemisphere Radiocarbon
1084 Age Calibration Curve (0–55 cal kBP). Radiocarbon 62, 725–757.
1085 Rijal, D.P., Heintzman, P.D., Lammers, Y., Yoccoz, N.G., Lorberau, K.E., Pitelkova, I., Goslar, T.,
1086 Murguzur, F.J.A., Sakari Salonen, J., Helmens, K.F., Bakke, J., Edwards, M.E., Alm, T., Bråthen,
1087 K.A., Brown, A.G., Alsos, I.G., 2020. Holocene plant diversity revealed by ancient DNA from 10
1088 lakes in northern Fennoscandia. Cold Spring Harbor Laboratory.
1089 https://doi.org/10.1101/2020.11.16.384065
1090 Roy, N., Bhiry, N., Woollett, J., Fréchette, B., 2018. Vegetation history since the mid-Holocene in
1091 northeastern Iceland. Écoscience 25, 109–123.
1092 Rundgren, M., 1998. Early-Holocene vegetation of northern Iceland: pollen and plant macrofossil
1093 evidence from the Skagi peninsula. Holocene 8, 553–564.
1094 Rundgren, M., 1997. Late Weichselian and early Holocene changes of vegetation, climate and sea
1095 level on the Skagi peninsula, northern Iceland (PhD). University of Lund, Lund.
1096 Rundgren, M., 1995. Biostratigraphic Evidence of the Allerød-Younger Dryas-Preboreal Oscillation in
1097 Northern Iceland. Quat. Res. 44, 405–416.
1098 Rundgren, M., Ingólfsson, O., 1999. Plant survival in Iceland during periods of glaciation? J.

1099 Biogeogr. 26, 387–396.
1100 Sæmundsson, T., 1995. Deglaciation and shoreline displacement in Vopnafjörður, North-eastern
1101 Iceland (PhD). University of Lund, Lund.
1102 Savile, D.B.O., 1972. Arctic adaptations in plants. Canada department of agriculture Research Branch
1103 Monograph 6, 1–81.
1104 Schaefer, H., 2003. Chorology and diversity of the Azorean flora. Stuttgart, J. Cramer.
1105 Smith, K.P., 1995. Landnám: The settlement of Iceland in archaeological and historical perspective.
1106 World Archaeol. 26, 319–347.
1107 Sohmer, S.H., Gustafson, R., 1987. Plants and flowers of Hawaii. Times Edition, Honolulu.
1108 Soininen, E.M., Gauthier, G., Bilodeau, F., Berteaux, D., Gielly, L., Taberlet, P., Gussarova, G.,
1109 Bellemain, E., Hassel, K., Stenøien, H.K., Epp, L., Schrøder-Nielsen, A., Brochmann, C.,
1110 Yoccoz, N.G., 2015. Highly overlapping diet in two sympatric lemming species during winter
1111 revealed by DNA metabarcoding. PLoS One 10, e0115335.
1112 Sønstebø, J.H., Gielly, L., Brysting, A.K., Elven, R., Edwards, M., Haile, J., Willerslev, E., Coissac,
1113 E., Rioux, D., Sannier, J., Taberlet, P., Brochmann, C., 2010. Using next-generation sequencing
1114 for molecular reconstruction of past Arctic vegetation and climate. Mol. Ecol. Resour. 10, 1009–
1115 1018.
1116 Stace, C.A., 1997. New Flora of the British Isles, 2nd ed. Cambridge University Press, Cambridge.
1117 Stewart, L., Alsos, I.G., Bay, C., Breen, A.L., Brochmann, C., Boulanger-Lapointe, N., Broennimann,
1118 O., Bültmann, H., Bøcher, P.K., Damgaard, C., Daniëls, F.J.A., Ehrich, D., Eidesen, P.B., Guisan,
1119 A., Jónsdóttir, I.S., Lenoir, J., le Roux, P.C., Lévesque, E., Luoto, M., Nabe-Nielsen, J.,
1120 Schönswetter, P., Tribsch, A., Tveraabak, L.U., Virtanen, R., Walker, D.A., Westergaard, K.B.,
1121 Yoccoz, N.G., Svenning, J.-C., Wisz, M., Schmidt, N.M., Pellissier, L., 2016. The regional
1122 species richness and genetic diversity of Arctic vegetation reflect both past glaciations and
1123 current climate. Glob. Ecol. Biogeogr. 25, 430–442.
1124 Svenning, J.-C., Eiserhardt, W.L., Normand, S., Ordonez, A., Sandel, B., 2015. The influence of
1125 paleoclimate on present-day patterns in biodiversity and ecosystems. Annu. Rev. Ecol. Evol.
1126 Syst. 46, 551–572.

1127 Taberlet, P., Coissac, E., Pompanon, F., Gielly, L., Miquel, C., Valentini, A., Vermat, T., Corthier, G.,
1128 Brochmann, C., Willerslev, E., 2007. Power and limitations of the chloroplast trnL (UAA) intron
1129 for plant DNA barcoding. Nucleic Acids Res. 35, e14.
1130 Thomas, P.A., El-Barghathi, M., Polwart, A., 2007. Biological Flora of the British Isles: *Juniperus*
1131 *communis* L. J. Ecol. 95, 1404–1440.
1132 Tollefsrud, M.M., Bachmann, K., Jakobsen, K.S., Brochmann, C., 1998. Glacial survival does not
1133 matter - II: RAPD phylogeography of Nordic *Saxifraga cespitosa*. Mol. Ecol. 7, 1217–1232.
1134 Verhoeven, K., Louwye, S., 2015. The Pleistocene palaeoenvironment and stratigraphy of Flatey
1135 island (northern Iceland): a preliminary assessment based on palynomorphs. Boreas 44, 588–602.
1136 Vésteinsson, O., McGovern, T.H., 2012. The Peopling of Iceland. Norwegian Archaeological Review
1137 45, 206–218.
1138 Voldstad, L.H., Alsos, I.G., Farnsworth, W.R., Heintzman, P.D., Håkansson, L., Kjellman, S.E.,
1139 Rouillard, A., Schomacker, A., Eidesen, P.B., 2020. A complete Holocene lake sediment ancient
1140 DNA record reveals long-standing high Arctic plant diversity hotspot in northern Svalbard. Quat.
1141 Sci. Rev. 234, 106207.
1142 Vorren, K.D., 1986. The impact of early agriculture on the vegetation of Northern Norway. A
1143 discussion of anthropogenic indicators in biostratigraphical data, in: Behre, K.-E. (Ed.),
1144 Anthropogenic Indicators in Pollen Idagrams. A.A.Balkema, Rotterdam, pp. 1–18.
1145 Wąsowicz, P., 2020. Annotated checklist of vascular plants of Iceland. Fjölrit Náttúrufræðistofnunar.
1146 https://doi.org/10.33112/1027-832x.57
1147 Wasowicz, P., Przedpelska-Wasowicz, E.M., Kristinsson, H., 2013. Alien vascular plants in Iceland:
1148 Diversity, spatial patterns, temporal trends, and the impact of climate change. Flora -
1149 Morphology, Distribution, Functional Ecology of Plants 208, 648–673.
1150 Weigelt, P., Steinbauer, M.J., Cabral, J.S., Kreft, H., 2016. Late Quaternary climate change shapes
1151 island biodiversity. Nature advance online publication. https://doi.org/10.1038/nature17443
1152 http://www.nature.com/nature/journal/vaop/ncurrent/abs/nature17443.html#supplementary-
1153 information
1154 Westergaard, K.B., Jørgensen, M.H., Gabrielsen, T.M., Alsos, I.G., Brochmann, C., 2010. The

1155 extreme Beringian/Atlantic disjunction in *Saxifraga rivularis* (Saxifragaceae) has formed at least
1156 twice. J. Biogeogr. 37, 1262–1276.
1157 Willerslev, E., Davison, J., Moora, M., Zobel, M., Coissac, E., Edwards, M.E., Lorenzen, E.D.,
1158 Vestergard, M., Gussarova, G., Haile, J., Craine, J., Gielly, L., Boessenkool, S., Epp, L.S.,
1159 Pearman, P.B., Cheddadi, R., Murray, D., Bråthen, K.A., Yoccoz, N., Binney, H., Cruaud, C.,
1160 Wincker, P., Goslar, T., Alsos, I.G., Bellemain, E., Brysting, A.K., Elven, R., Sonstebo, J.H.,
1161 Murton, J., Sher, A., Rasmussen, M., Ronn, R., Mourier, T., Cooper, A., Austin, J., Moller, P.,
1162 Froese, D., Zazula, G., Pompanon, F., Rioux, D., Niderkorn, V., Tikhonov, A., Savvinov, G.,
1163 Roberts, R.G., MacPhee, R.D.E., Gilbert, M.T.P., Kjaer, K.H., Orlando, L., Brochmann, C.,
1164 Taberlet, P., 2014. Fifty thousand years of Arctic vegetation and megafaunal diet. Nature 506,
1165 47–51.
1166 Xiao, X., Zhao, M., Knudsen, K.L., Sha, L., Eiríksson, J., Gudmundsdóttir, E., Jiang, H., Guo, Z.,
1167 2017. Deglacial and Holocene sea–ice variability north of Iceland and response to ocean
1168 circulation changes. Earth Planet. Sci. Lett. 472, 14–24.
1169 Þórhallsdóttir, Þ.E., 1996. Áhrif búsetu á landið, in: Grímsdóttir, G.Á. (Ed.), Um Landnám á Íslandi –
1170 Fjórtán Erindi. Vísindafélag Íslendinga, Reykjavik.

1171

Tables

Table 1. Radiocarbon ages from Torfdalsvatn (TDV) and Nykurvatn (NYK). Calibrated ages are median ages within the 2σ age ranges.

Core	Original depth (cm)	Composite depth (cm)	Lab ID	^{14}C age (yr BP)	Calibrated age (cal. yr BP)	Calibrated 2σ age ranges (cal. yr BP)	δ^{13}C (‰ VPDB)	Dated material
TDV2-1	78-79	78-79	Ua-67062	439 ± 27	501	529-463	-11.6	*Equisetum*
TDV2-2	5-6	130-131	Ua-67063	1159 ± 28	1065	1178-972	-11.9	Graminoid
TDV2-2	44-45	169-170	Ua-67064	1419 ± 28	1323	1356-1290	-8.6	Twig
TDV2-3	49-50	314-315	Ua-67065	2192 ± 29	2232	2314-2118	-9.3	*Equisetum*?
TDV2-4	85-86	491-492	Ua-67066	3603 ± 30	3909	4061-3832	-9.5	Graminoid
TDV2-6	15-16	708-709	Ua-67067	5819 ± 33	6628	6733-6500	-10.1	Graminoid
NYK1	48-49	48-49	Ua-65341	3597 ± 31	3902	3984-3778	-23.9	Twig (*Betula* sp.)
NYK1	103-104	103-104	Ua-67058	1211 ± 28	1128	1247-1061	-14.6	Moss
NYK4	71-72	268-269	Ua-67060	5091 ± 32	5812	5915-5746	-28.9	Twig
NYK3	143-144	270-271	Ua-67059	5021 ± 34	5773	5895-5658	-19.9	Moss
NYK5	62-63	380-381	Ua-65343	6125 ± 45	7009	7160-6890	–	Leaf (*Betula nana*/sp.)
NYK5	80.5-81.5	398-399	Ua-67061	6909 ± 35	7734	7834-7670	-26.6	Twig (*Salix* sp.)
NYK5	133-134	451-452	Ua-65344	7511 ± 38	8335	8391-8199	-28.0	Leaf (*Salix herbacea*)

1177 Table 2. Identified tephra marker layers from Torfdalsvatn (TDV) and Nykurvatn (NYK),

1178 used for the age-depth models. H = Historical; R = Radiocarbon; I = Ice core.

Tephra layer name (core, composite depth)	Volcanic system	Silicic (S) Basaltic (B)	Tephra marker	Age (cal. yr BP)	Age (yr BP)	Type of date	Reference for age
NYK61	Veiðivötn-Bárðarbunga	B	V1477	470	-	H	(Larsen et al., 2002)
TDV115	Hekla	S	Hekla 1104	850	-	H	(Larsen et al., 2002)
TDV407, NYK136	Hekla	S	Hekla 3	3005 ± 57	2879 ± 34	R	(Dugmore et al., 1995)
TDV505, NYK198	Hekla	S	Hekla 4	4196 ± 33	3826 ± 12	R	(Dugmore et al., 1995)
TDV839	Grímsvötn	B	Saksunarvatn Ash	10267 ± 89	-	I	(Rasmussen et al., 2006)

1179

1180

1181

Figure legends

Fig. 1. A. Overview map of the Arctic. Iceland is marked in black. B. Map of Iceland. The box indicates the extent of C. C. Terrain shaded relief map of Northeast Iceland showing the location of the two study areas. D. The area around Torfdalsvatn shown on an aerial orthophotograph. E. The area around Nykurvatn shown on an aerial orthophotograph. The imagery in C-E is available from the National Land Survey of Iceland (2020).

Fig. 2. Catchment overviews of Torfdalsvatn (A-B), and Nykurvatn (C-D). Photographs taken June 2013 (G. Gísladóttir) and July 2017 (Í.Ö. Benediktsson), respectively.

Fig. 3. Age-depth models for Torfdalsvatn (A), and Nykurvatn (B). Details for all radiocarbon ages are given in Table 1 and tephra marker layers in Table 2 and Supplementary Table S1.

Fig. 4. Lithology, depths for *sed*aDNA samples, identified tephra marker layers and calibrated median ages for (A) Torfdalsvatn (TDV) and (B) Nykurvatn (NYK). In addition, magnetic susceptibility (MS) and Ti/(inc+coh) are presented for TDV, and LOI (%) and Ti/Sum for NYK.

Fig. 5. Taxa identified in the *sed*aDNA metabarcoding analyses sorted according to plant functional group (colour bars) and arrival time for Torfdalsvatn, Iceland. All data shown as occurrence in weighted proportion of 8 PCR repeats (see methods). Assumed naturalised non-native taxa are in red and with a star after the name. Zonation according to CONISS analyses are shown with black lines, lithological units with black broken lines and the Saksunarvatn

tephra in grey line. Note that some taxa names are shortened. See Supplementary Table S4 for full taxa list.

Fig. 6. Vegetation development shown as proportion of reads for each functional group. The proportion of terrestrial and aquatic reads is shown for Torfdalsvatn (A) and Nykurvatn (B), along with the proportion of unidentified and partially identified reads. The proportion of reads for terrestrial functional groups is shown for Torfdalsvatn (C) and Nykurvatn (D). For Nykurvatn, the bryophytes, graminoids and cryptogams have average read proportions <0.01 and thus are not clearly visible. Vertical lines in A and C denote the *sed*aDNA zones according to CONISS analyses.

Fig. 7. Taxa identified in the *sed*aDNA metabarcoding analyses sorted according to plant functional group (colour bars) and arrival time for Nykurvatn. All data shown as occurrence in weighted proportion of 8 PCR repeats (see methods). One assumed naturalised non-native taxon is in red and with a star after the name. Note that some taxa names are shortened. See Supplementary Table S4 for full taxa list.

Fig. 8. Development in species richness, local and regional species pools in Iceland. Species pool (defined as cumulative number of taxa) per functional type for Torfdalsvatn (A), Nykurvatn (B), and both sites combined with the macrofossil and pollen data from Alsos et al., 2016 (C). Vertical lines in A denote the *sed*aDNA zones according to CONISS analyses, while the vertical lines in C indicate the start of the Torfdalsvatn and Nykurvatn cores. (D) Accumulated detected regional species pool as well as number of taxa detected per sample along with the 95% confidence interval (grey shading) of the fitted line. Open circles represent excluded samples, which were not used for the richness curves (Supplementary

Table S6). The regional species pool is the data from both sites combined, along with the macrofossil and pollen data from (Alsos et al., 2016).

Fig. 9. Lithology, *sed*aDNA zones from the CONISS analyses, magnetic susceptibility (MS, Torfdalsvatn only), loss on ignition (LOI, Nykurvatn only), species richness, proportion of reads for terrestrial plants, proportion of reads for trees and shrubs, and number of new taxa recorded per 500 years (new taxa from both sites and Alsos et al., 2016) compared to regional paleoclimate records. The IP_{25} biomarker record is a proxy for sea ice from two marine sediment cores at the North Iceland shelf (MD99-2269, Cabedo-Sanz et al., 2016; MD99-2272, Xiao et al., 2017, note that even 11,000-7000 cal. yr BP, some sea ice was present NE of Iceland occasionally connecting Iceland to N Scandianvia/Russia, Alsos et al., 2016). The mean summer air temperature anomaly is based on the biomarker brGDGT from Skorarvatn, Northwest Iceland (Harning et al., 2020). Grey shading indicates the propagated standard error. The key to the lithology is given in Fig. 4. Results from Torfdalsvatn (A) and Nykurvatn (B).

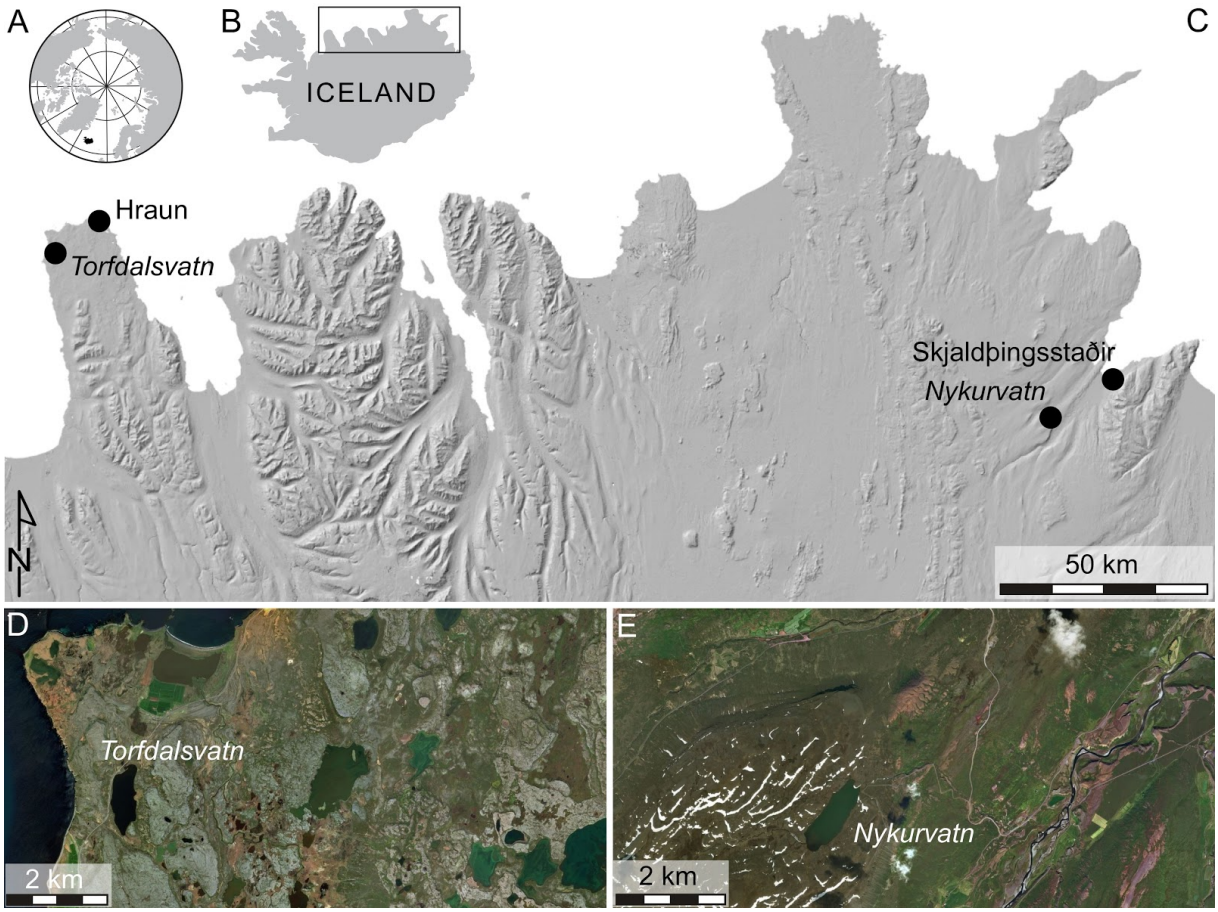
A
B
ICELAND
C
Hraun
Torfdalsvatn
Skjaldþingsstaðir
Nykurvatn
N
50 km
D
Torfdalsvatn
2 km
E
Nykurvatn
2 km

Fig 1

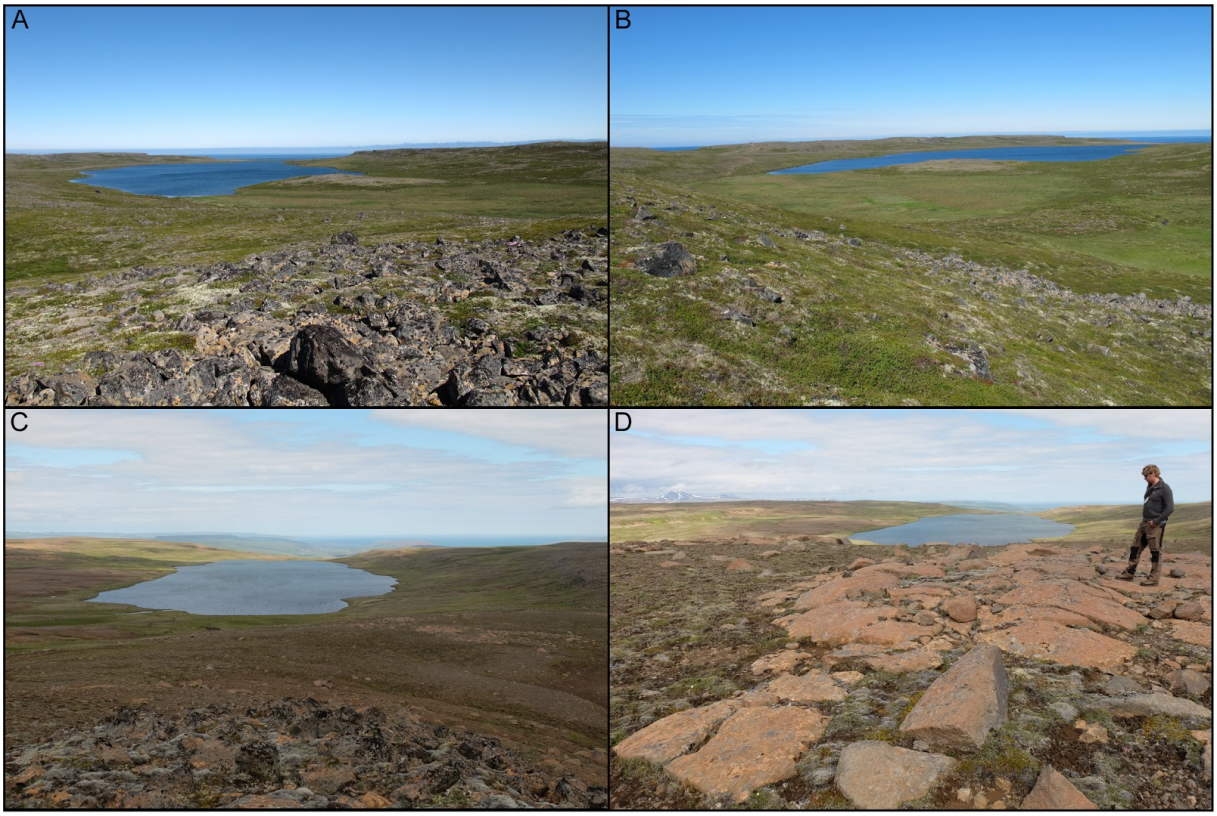

Fig. 2

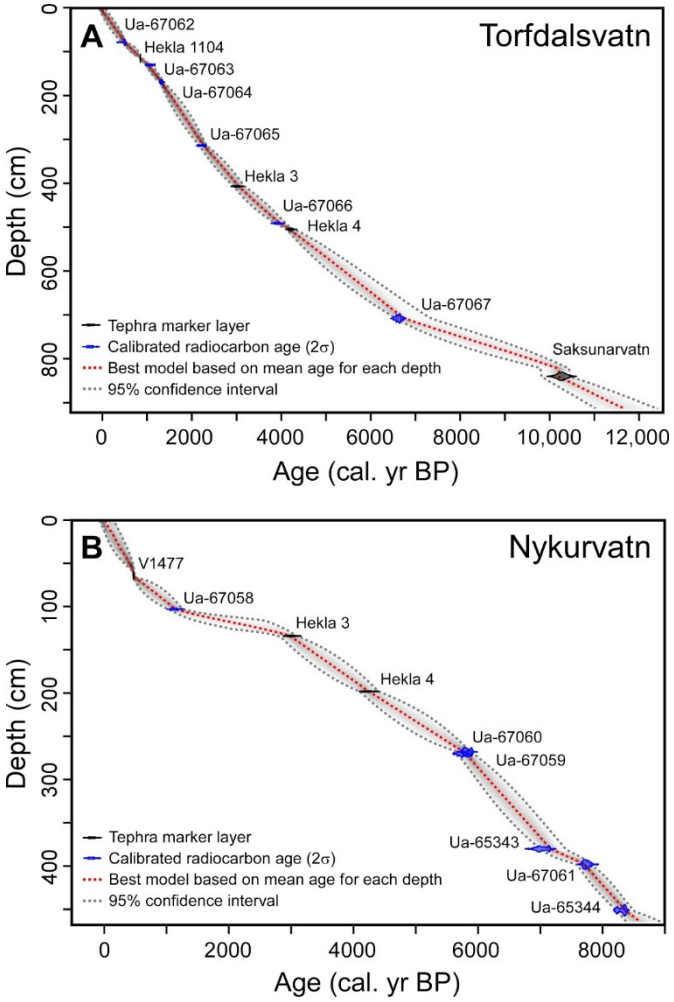
A
Torfdalsvatn
Ua-67062
Hekla 1104
Ua-67063
Ua-67064
Ua-67065
Hekla 3
Ua-67066
Hekla 4
Ua-67067
Saksunarvatn
Tephra marker layer
Calibrated radiocarbon age (2σ)
Best model based on mean age for each depth
95% confidence interval
Depth (cm)
0
200
400
600
800
0
2000
4000
6000
8000
10,000
12,000
Age (cal. yr BP)
B
Nykurvatn
V1477
Ua-67058
Hekla 3
Hekla 4
Ua-67060
Ua-67059
Ua-65343
Ua-67061
Ua-65344
Tephra marker layer
Calibrated radiocarbon age (2σ)
Best model based on mean age for each depth
95% confidence interval
Depth (cm)
0
100
200
300
400
0
2000
4000
6000
8000
Age (cal. yr BP)

Fig. 3

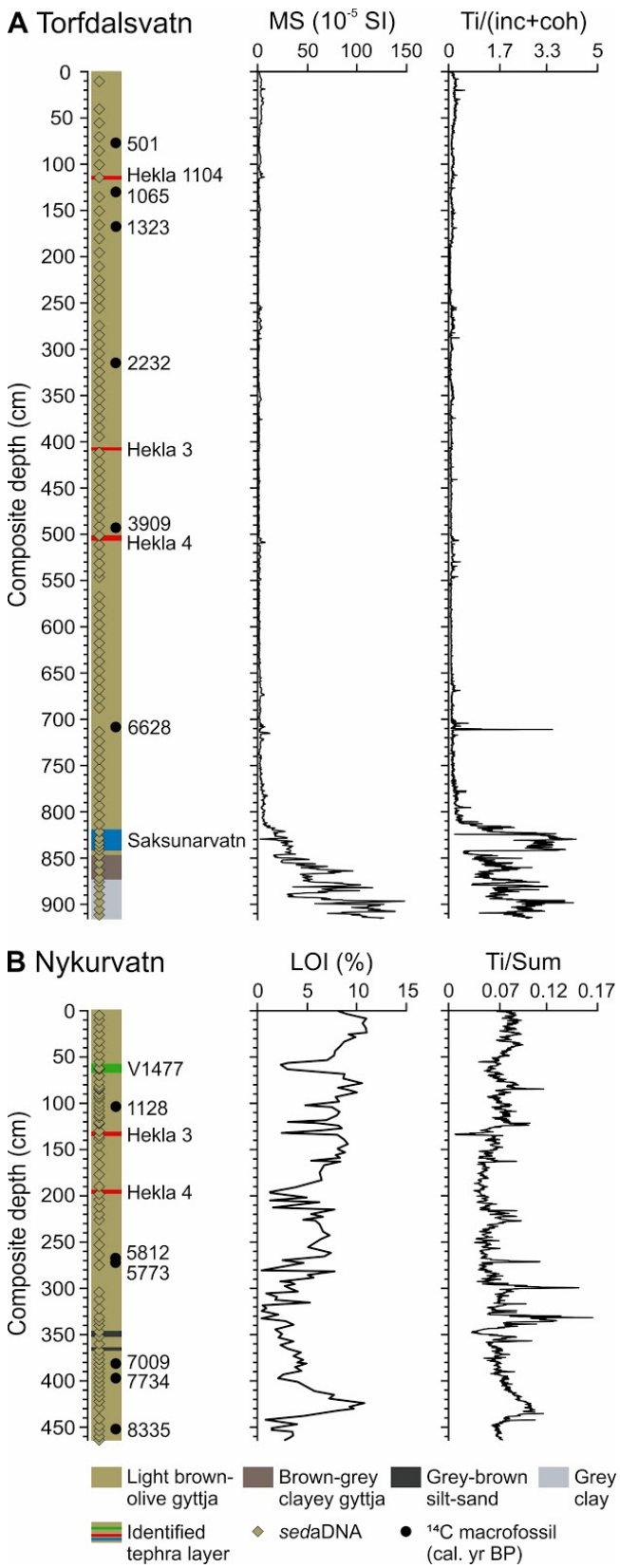
A Torfdalsvatn
MS (10-5 SI)
Ti/(inc+coh)
Composite depth (cm)
501
Hekla 1104
1065
1323
2232
Hekla 3
3909
Hekla 4
6628
Saksunarvatn
B Nykurvatn
LOI (%)
Ti/Sum
V1477
1128
Hekla 3
Hekla 4
5812
5773
7009
7734
8335
Light brown-olive gyttja
Brown-grey clayey gyttja
Grey-brown silt-sand
Grey clay
Identified tephra layer
sedaDNA
14C macrofossil (cal. yr BP)

Fig. 4

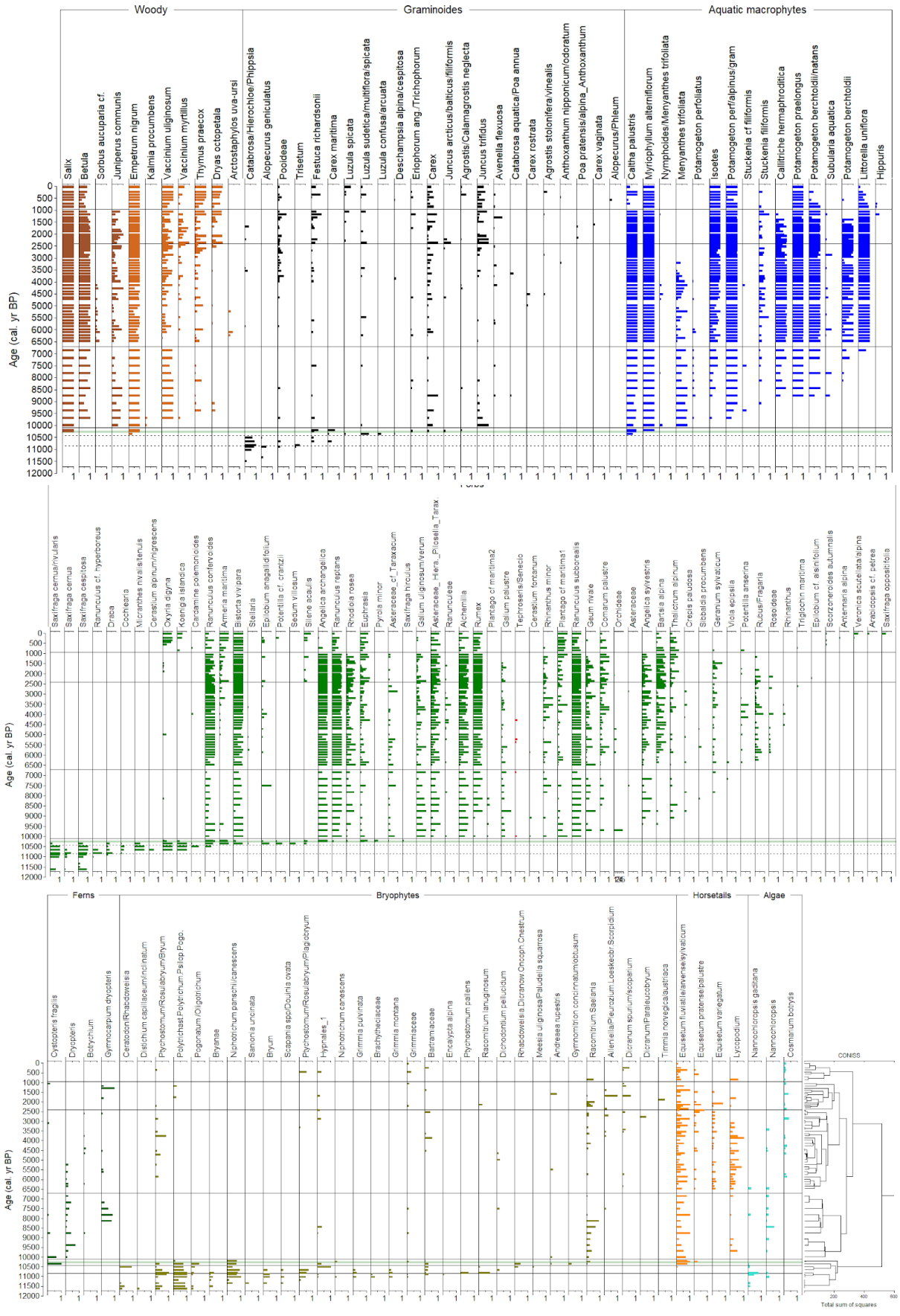
Woody
Graminoides
Aquatic macrophytes
Ferns
Bryophytes
Horsetails
Algae
Age (cal. yr BP)
CONISS
Total sum of squares

Fig. 5

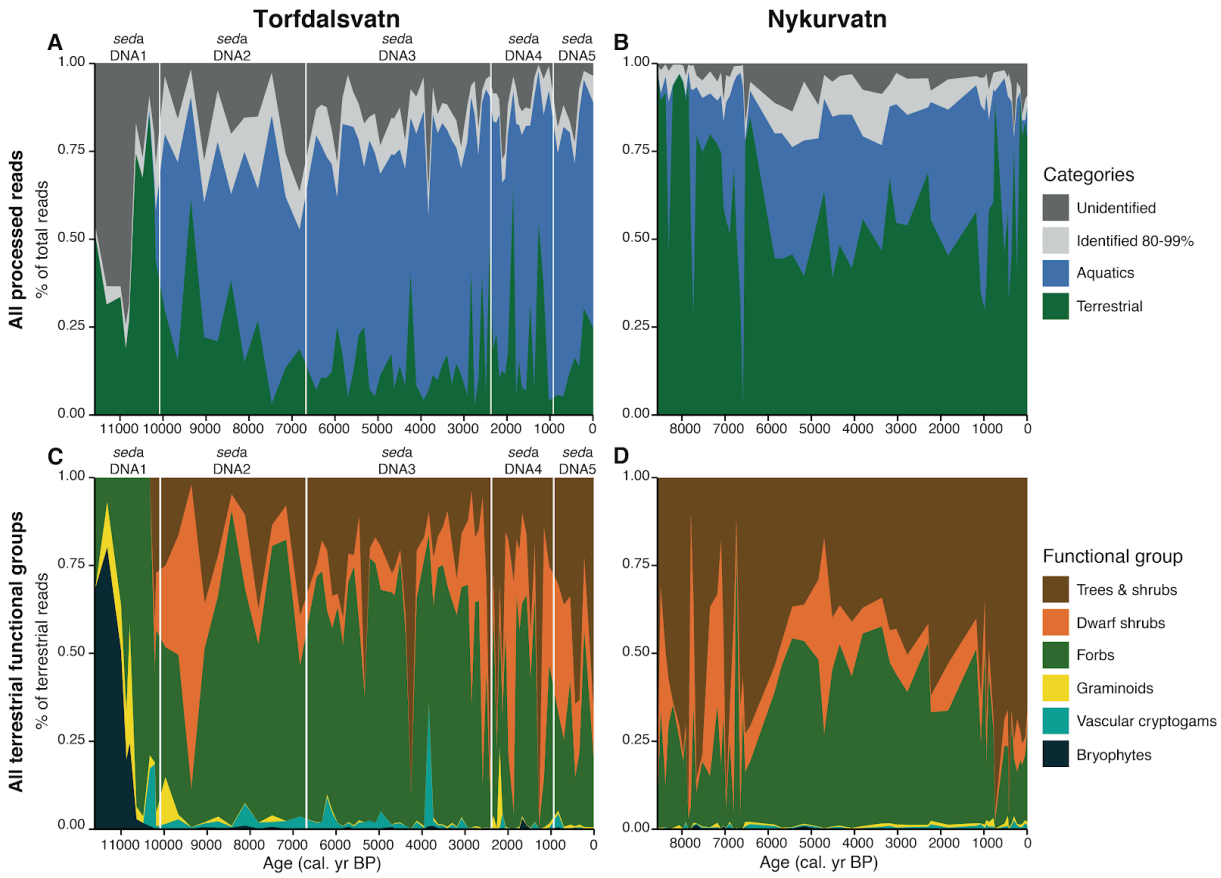
Torfdalsvatn
Nykurvatn
A
B
C
D
sedaDNA1
sedaDNA2
sedaDNA3
sedaDNA4
sedaDNA5
All processed reads
% of total reads
All terrestrial functional groups
% of terrestrial reads
Age (cal. yr BP)
Categories
Unidentified
Identified 80-99%
Aquatics
Terrestrial
Functional group
Trees & shrubs
Dwarf shrubs
Forbs
Graminoids
Vascular cryptogams
Bryophytes

Fig. 6

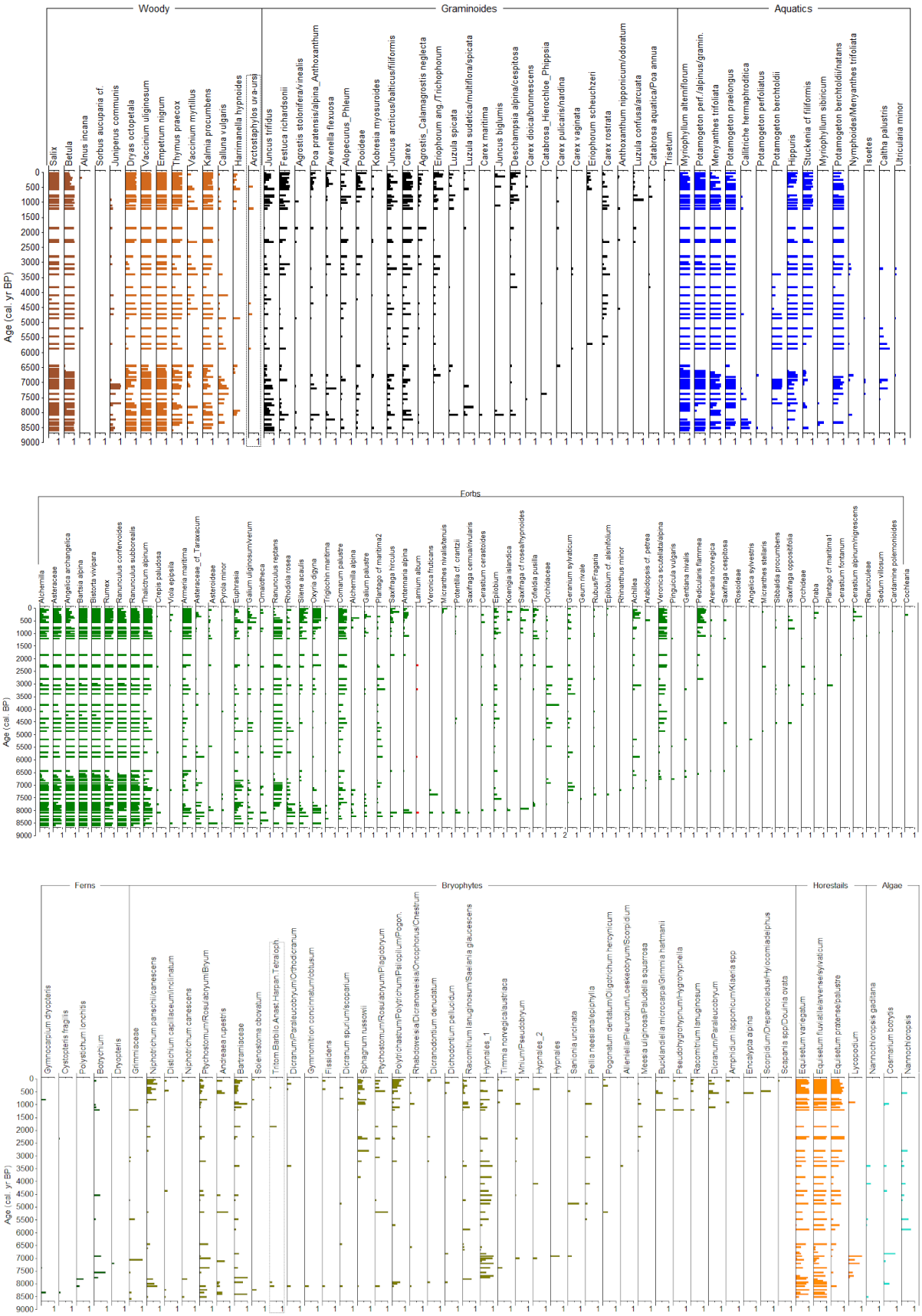
Woody
Graminoides
Aquatics
Forbs
Ferns
Bryophytes
Horestails
Algae
Age (cal. yr BP)
Salix
Betula
Alnus incana
Sorbus aucuparia cf.
Juniperus communis
Dryas octopetala
Vaccinium uliginosum
Empetrum nigrum
Thymus praecox
Vaccinium myrtillus
Kalmia procumbens
Calluna vulgaris
Harrimanella hypnoides
Arctostaphylos uva-ursi
Juncus trifidus
Festuca richardsonii
Agrostis stoloniferа/vinealis
Poa pratensis/alpina_Anthoxanthum
Avenella flexuosa
Alopecurus_Phleum
Pooideae
Kobresia myosuroides
Juncus arcticus/balticus/filiformis
Carex
Agrostis_Calamagrostis neglecta
Eriophorum ang./trichophorum
Luzula spicata
Luzula sudetica/multiflora/spicata
Carex maritima
Juncus biglumis
Deschampsia alpina/cespitosa
Carex dioica/brunnescens
Catabrosa_Hierochloe_Phippsia
Carex pulicaris/nardina
Carex vaginata
Eriophorum scheuchzeri
Carex rostrata
Anthoxanthum nipponicum/odoratum
Luzula confusa/arcuata
Catabrosa aquatica/Poa annua
Trisetum
Myriophyllum alterniflorum
Potamogeton perf./alpinus/gramin.
Menyanthes trifoliata
Potamogeton praelongus
Callitriche hermaphroditica
Potamogeton perfoliatus
Potamogeton berchtoldi
Hippuris
Stuckenia cf filiformis
Myriophyllum sibiricum
Potamogeton berchtoldi/natans
Nymphoides/Menyanthes trifoliata
Isoetes
Caltha palustris
Utricularia minor
Alchemilla
Asteraceae
Angelica archangelica
Bartsia alpina
Bistorta vivipara
Rumex
Ranunculus confervoides
Ranunculus subborealis
Thalictrum alpinum
Crepis paludosa
Viola epipsila
Armeria maritima
Asteraceae_cf_Taraxacum
Asteroideae
Pyrola minor
Euphrasia
Galium uliginosum/verum
Omalotheca
Ranunculus reptans
Rhodiola rosea
Silene acaulis
Oxyria digyna
Triglochin maritima
Comarum palustre
Alchemilla alpina
Galium palustre
Plantago cf maritima2
Saxifraga hirculus
Antennaria alpina
Lamium album
Veronica fruticans
Micranthes nivalis/tenuis
Potentilla cf. crantzii
Saxifraga cernua/rivularis
Cerastium cerastioides
Epilobium
Koenigia islandica
Saxifraga cf rosea/hyponoides
Tofieldia pusilla
Orchidaceae
Geranium sylvaticum
Geum rivale
Rubus/Fragaria
Epilobium cf. alsinifolium
Rhinanthus minor
Achillea
Arabidopsis cf. petrea
Veronica scutellata/alpina
Pinguicula vulgaris
Gentiana nivalis
Pedicularis flammea
Arenaria norvegica
Saxifraga cespitosa
Rosoideae
Angelica sylvestris
Micranthes stellaris
Sibbaldia procumbens
Saxifraga oppositifolia
Orchideae
Draba
Plantago cf maritima1
Cerastium fontanum
Cerastium alpinum/nigrescens
Ranunculeae
Sedum villosum
Cardamine polemonioides
Cochlearia
Gymnocarpium dryopteris
Cystopteris fragilis
Polystichum lonchitis
Botrychium
Dryopteris
Gymnocarpium jessoense/robertianum
Dicranum spurium/scoparium
Sphagnum russowii
Pleurozium schreberi
Polytrichastrum/Polytrichum/Pogonatum
Rhabdoweisia/Dicranoweisia/Oncophorus/Chesnetum
Dicranodontium denudatum
Dichodontium pellucidum
Racomitrium lanuginosum/Saelania glaucescens
Hypnales_1
Timmia norvegica/austriaca
Mnium/Pseudobryum
Hypnales_2
Hypnales
Sanionia uncinata
Pellia neesiana/epiphylla
Pogonatum dentatum/Oligotrichum hercynicum
Aulacomnium turgidum/palustre
Meesia uliginosa/Paludella squarrosa
Bucklandiella microcarpa/Grimmia hartmanii
Pseudohygrohypnum/Hygrohypnella
Racomitrium lanuginosum
Dicranum/Paraleucobryum
Amphidium lapponicum/Klazenia spp.
Encalypta alpina
Scorpidium/Drepanocladus/Hylocomiadelphus
Scapania spp/Diplophyllum obtusum
Equisetum variegatum
Equisetum fluviatile/arvense/sylvaticum
Equisetum pratense/palustre
Lycopodium
Nannochloropsis gaditana
Coelastrum botrytis
Nannochloropsis

Fig. 7

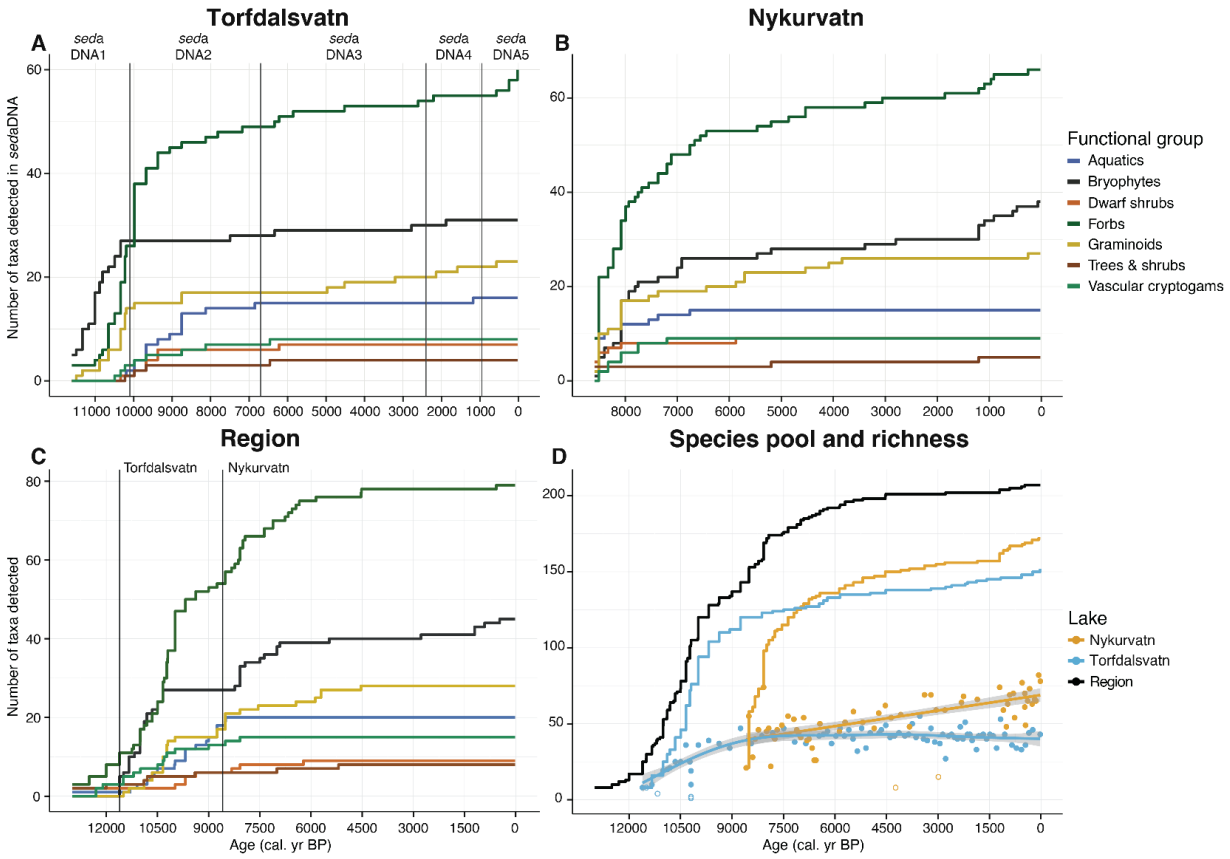
Torfdalsvatn
A
sedaDNA1
sedaDNA2
sedaDNA3
sedaDNA4
sedaDNA5
Number of taxa detected in sedaDNA
11000 10000 9000 8000 7000 6000 5000 4000 3000 2000 1000 0
Nykurvatn
B
8000 7000 6000 5000 4000 3000 2000 1000 0
Functional group
Aquatics
Bryophytes
Dwarf shrubs
Forbs
Graminoids
Trees & shrubs
Vascular cryptogams
Region
C
Torfdalsvatn
Nykurvatn
Number of taxa detected
12000 10500 9000 7500 6000 4500 3000 1500 0
Age (cal. yr BP)
Species pool and richness
D
Lake
Nykurvatn
Torfdalsvatn
Region

Fig. 8

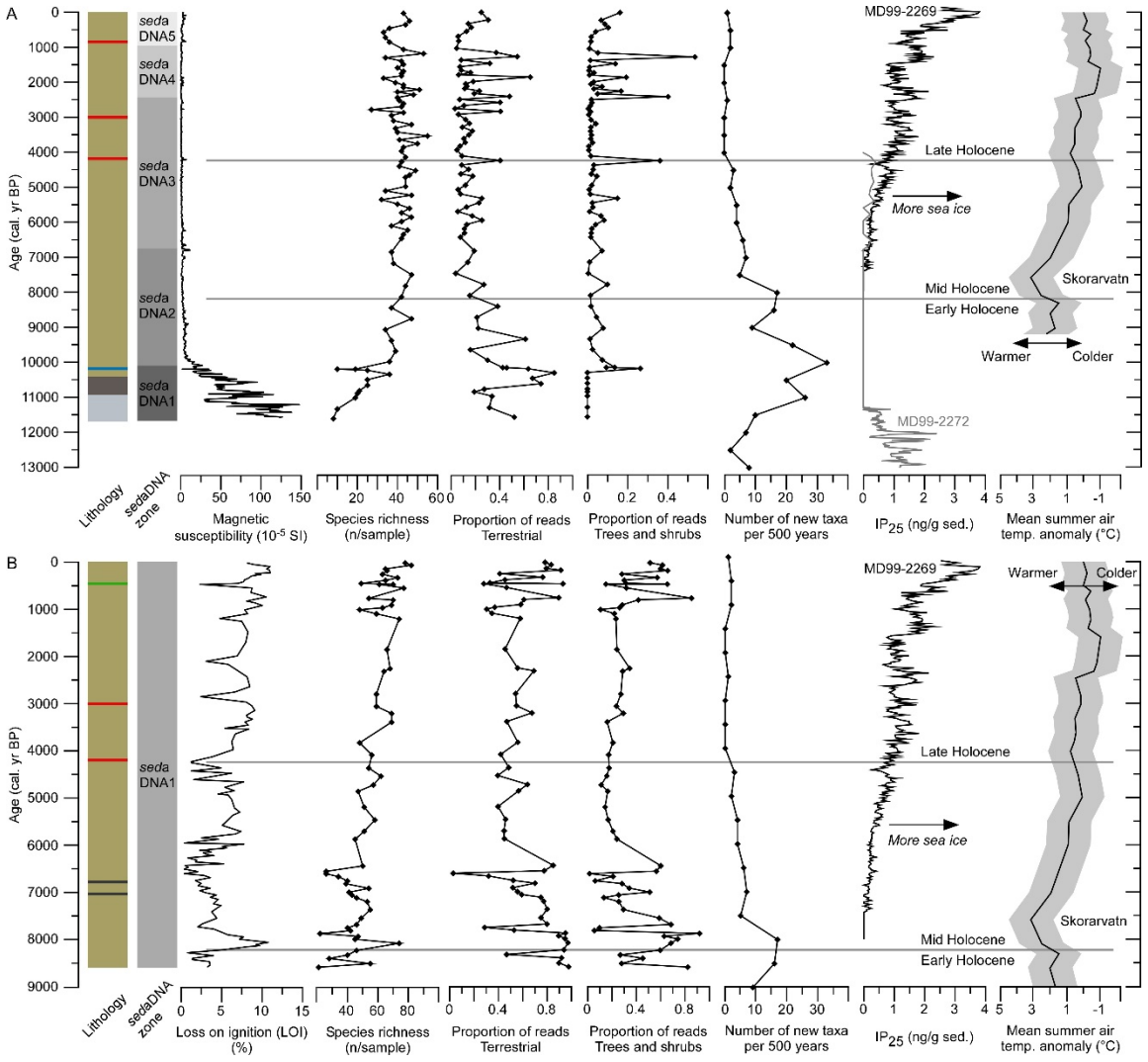
A
B
Age (cal. yr BP)
Lithology
sedaDNA zone
seda DNA5
seda DNA4
seda DNA3
seda DNA2
seda DNA1
Magnetic susceptibility (10-5 SI)
Loss on ignition (LOI) (%)
Species richness (n/sample)
Proportion of reads Terrestrial
Proportion of reads Trees and shrubs
Number of new taxa per 500 years
MD99-2269
MD99-2272
IP25 (ng/g sed.)
Mean summer air temp. anomaly (°C)
Late Holocene
Mid Holocene
Early Holocene
More sea ice
Skorarvatn
Warmer
Colder

Fig. 9